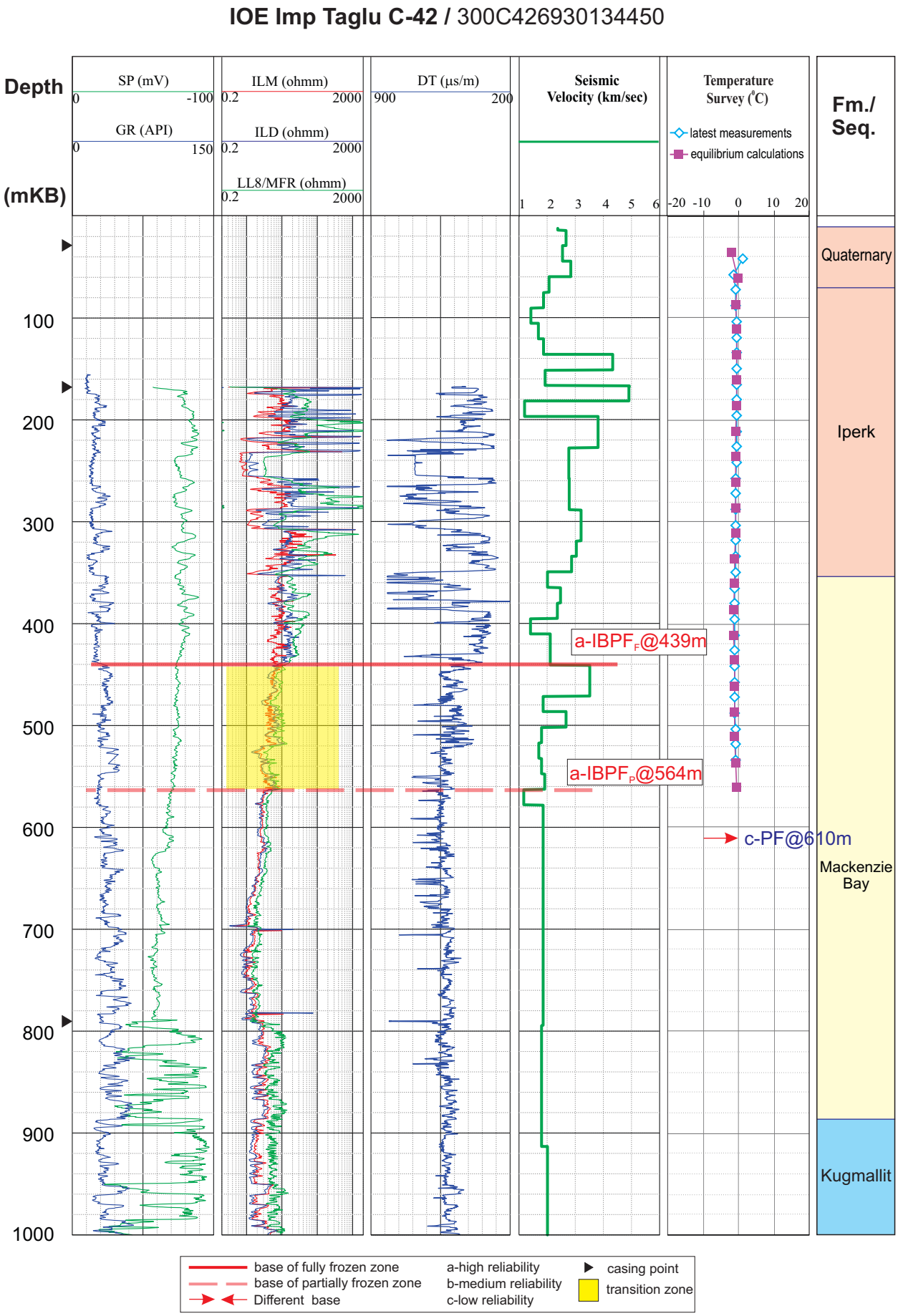

Figure 191. Determination of base of permafrost using temperature survey, well seismic survey and geophysical logs for the Taglu C-42 well in the Beaufort-Mackenzie Basin.

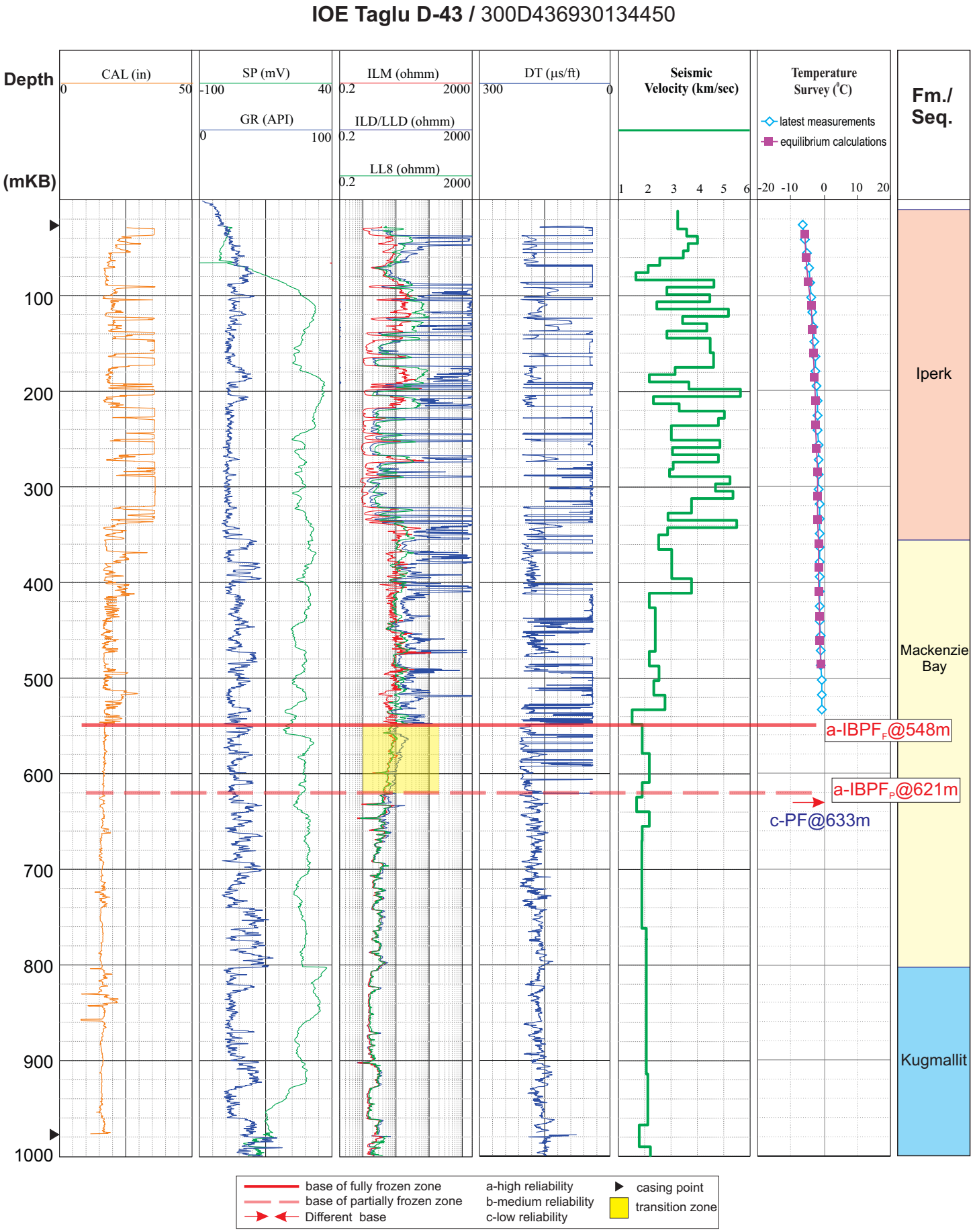

Figure 192. Determination of base of permafrost using temperature survey, well seismic survey and geophysical logs for the Taglu D-43 well in the Beaufort-Mackenzie Basin.

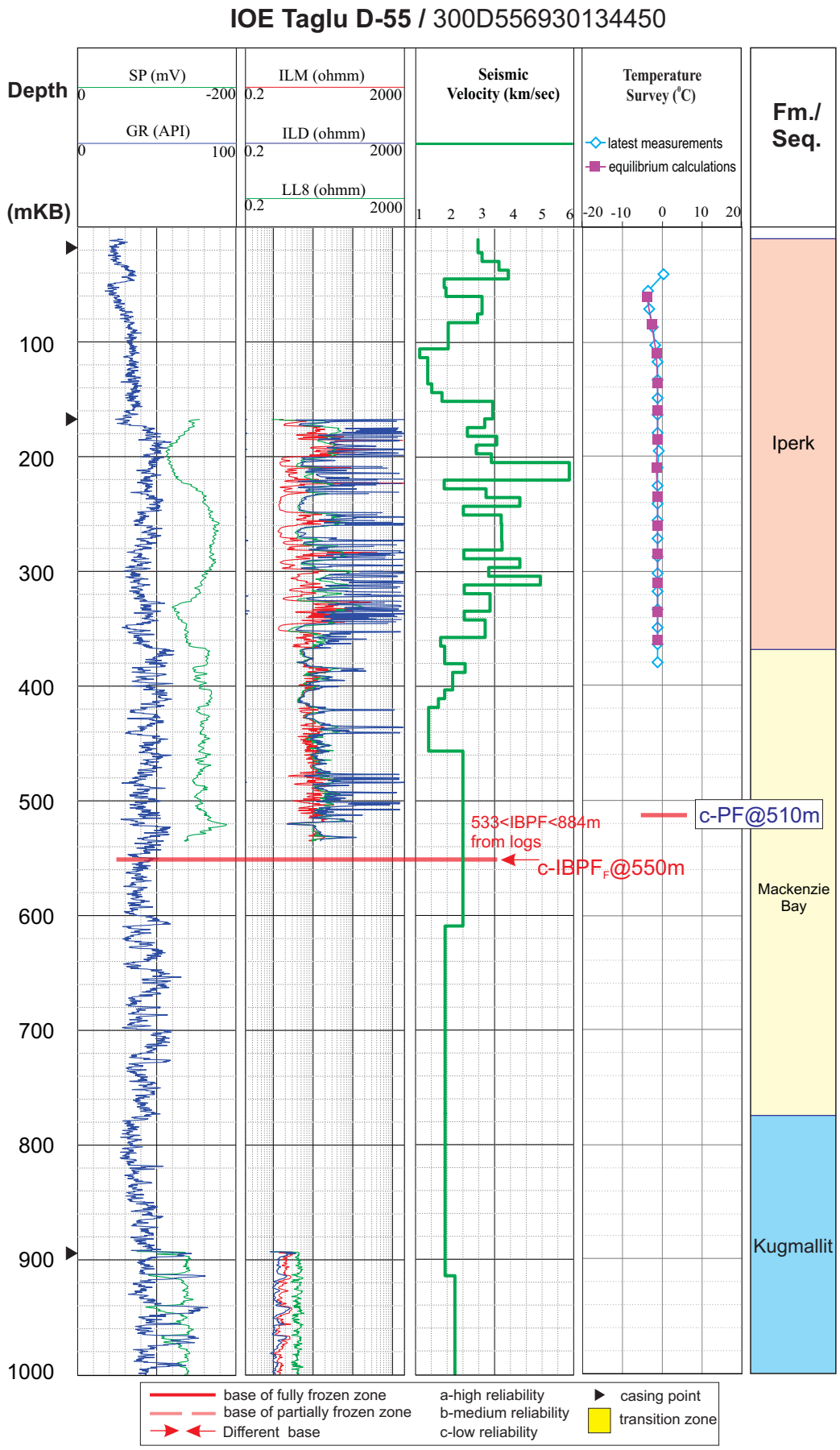

Figure 193. Determination of base of permafrost using temperature survey, well seismic survey and geophysical logs for the Taglu D-55 well in the Beaufort-Mackenzie Basin. The final IBPF pick is from temperature survey. Based on the logs, IBPF is less than 884m, and greater than 533m. Considering IBPF data of neighbor wells and the response trends of Gamma ray and resistivity, another possible IBPF could be around 550m (the red arrow).

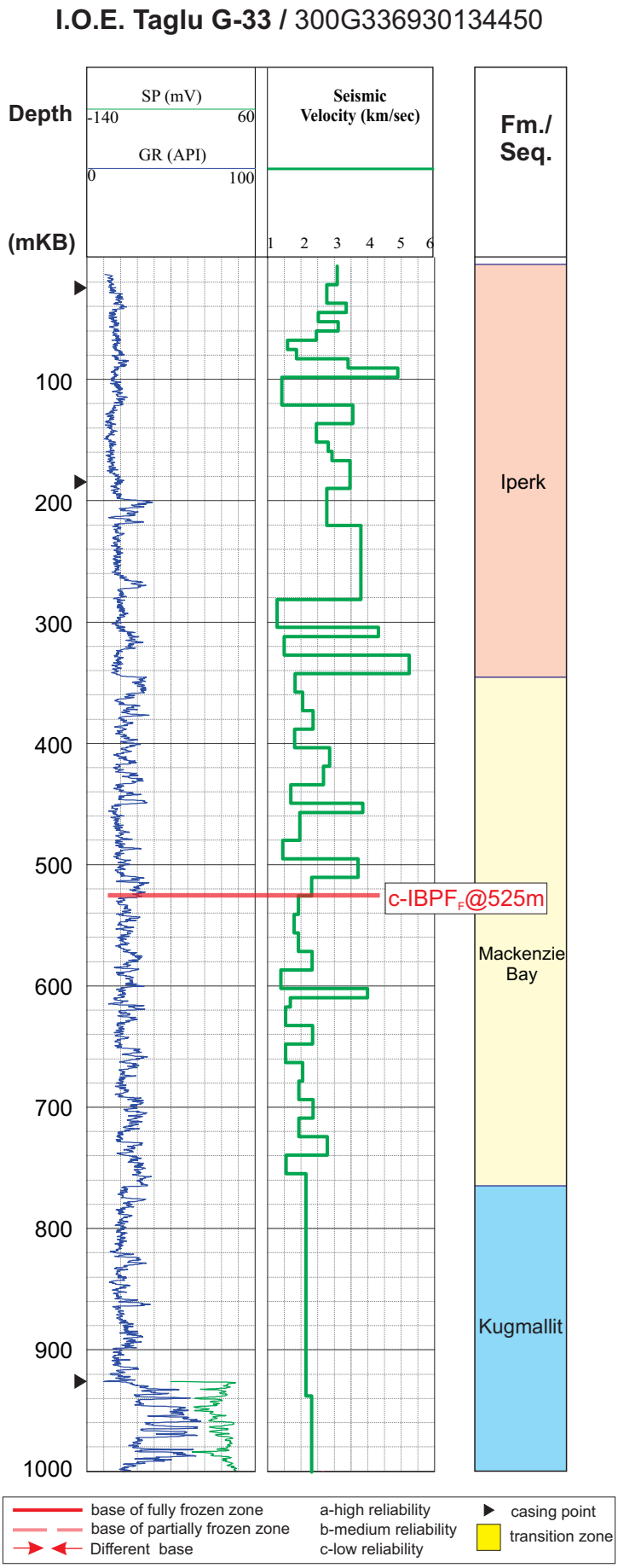

Figure 194. The base of permafrost is estimated mainly from well seismic survey for the Taglu G-33 well in the Beaufort-Mackenzie Basin.

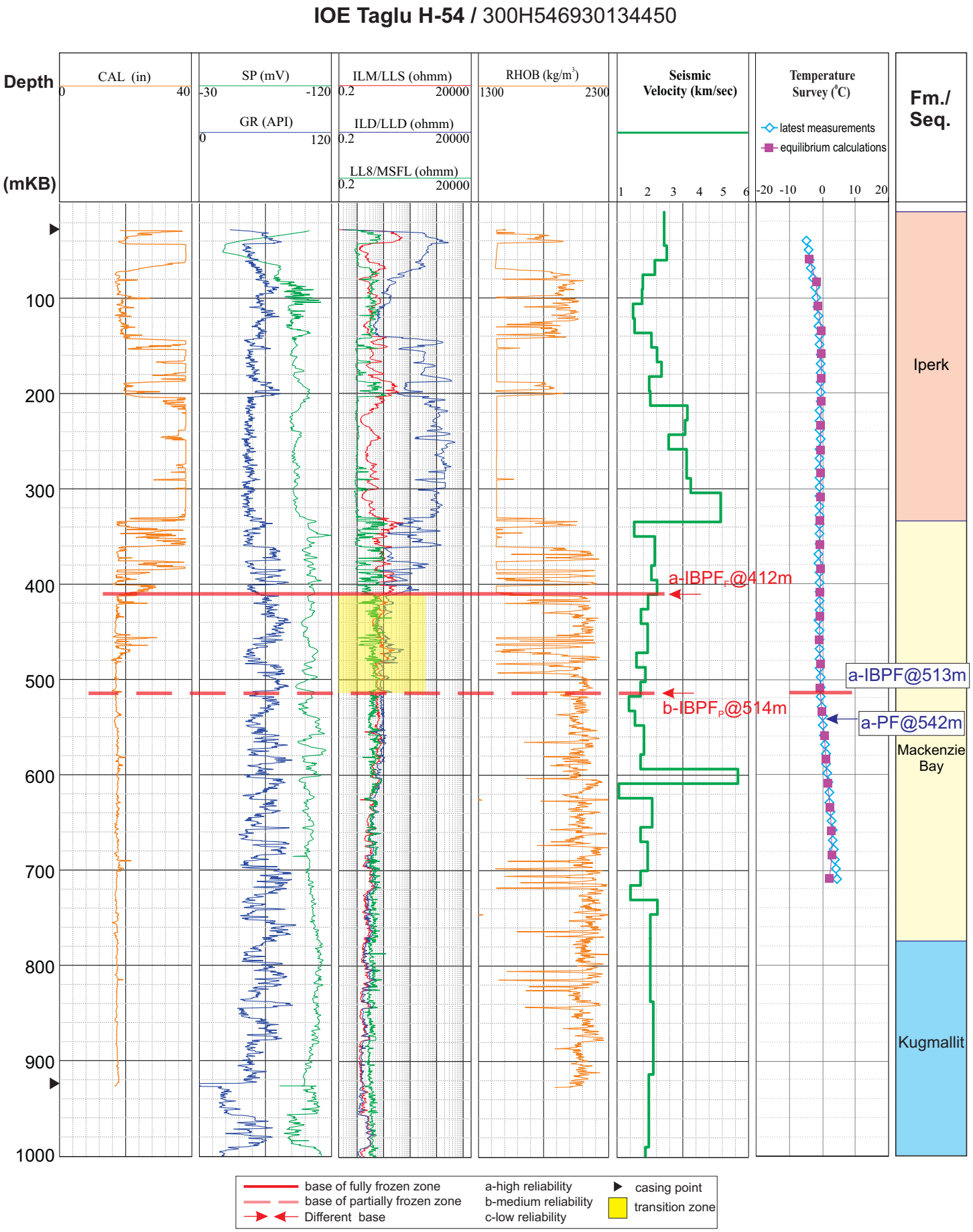

Figure 195. Determination of base of permafrost using temperature survey, well seismic survey and geophysical logs for the Taglu H-54 well in the Beaufort-Mackenzie Basin.

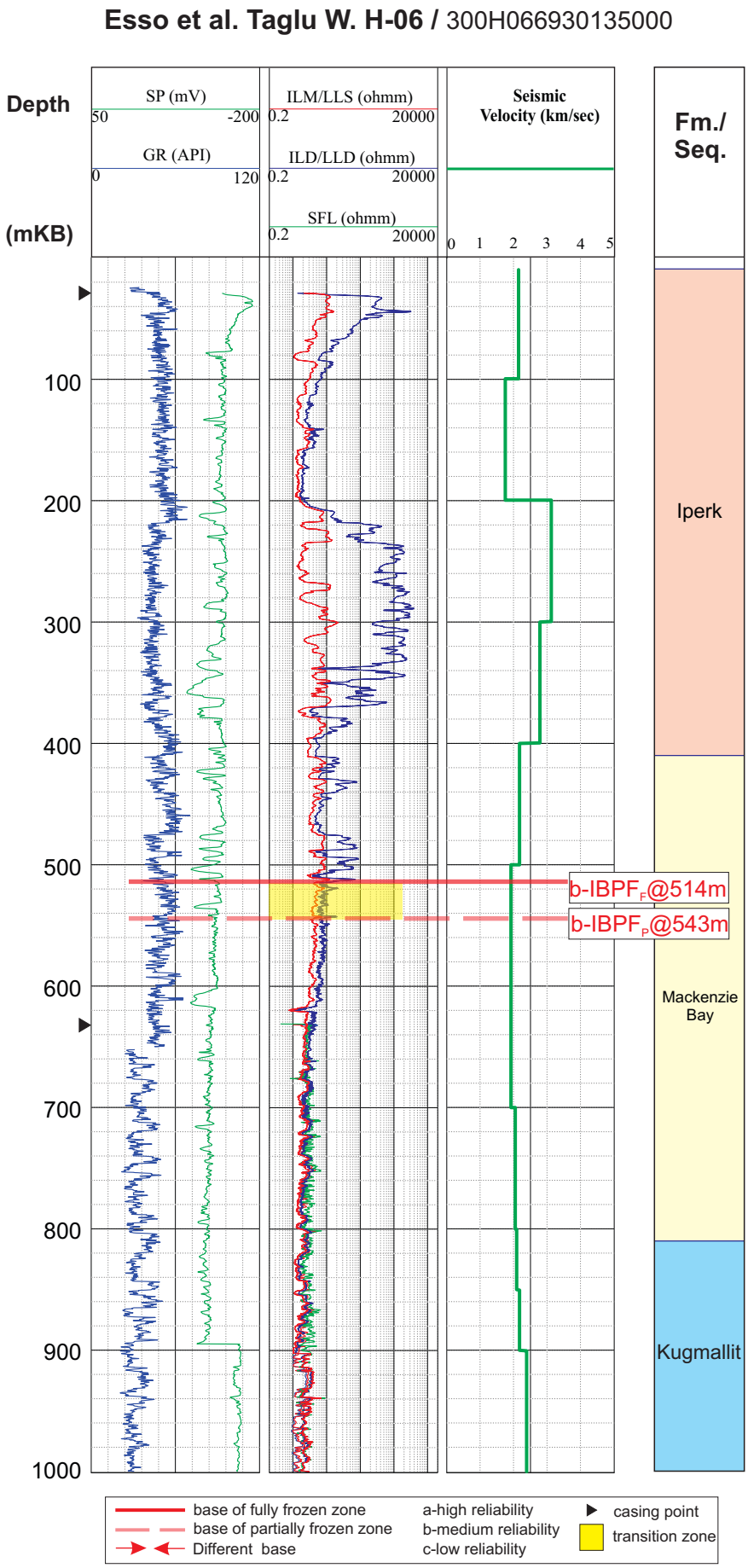

Figure 196. Determination of base of permafrost using well seismic survey and geophysical logs for the Taglu W. H-06 well in the Beaufort-Mackenzie Basin.

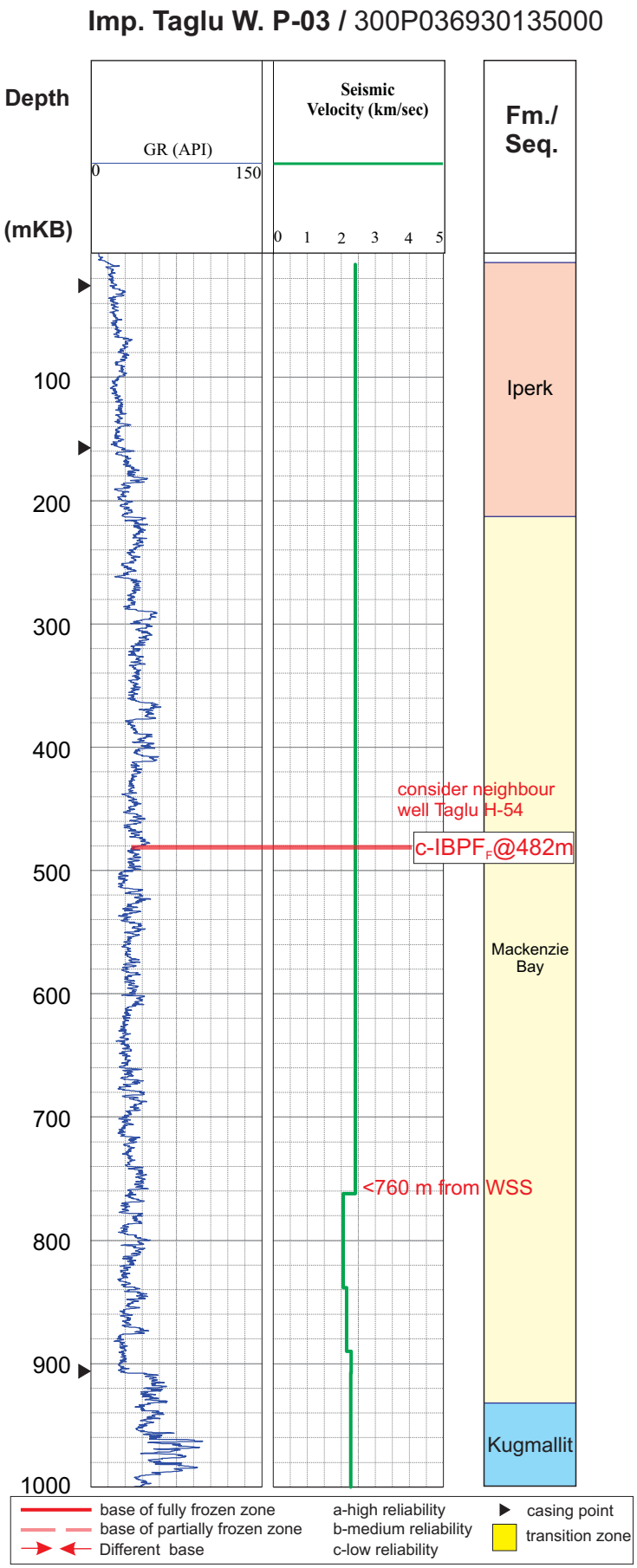

Figure 197. Estimation of base of permafrost using well seismic survey, gamma ray log, and IBPF data of neighbor well for the Taglu W. P-03 well in the Beaufort-Mackenzie Basin.

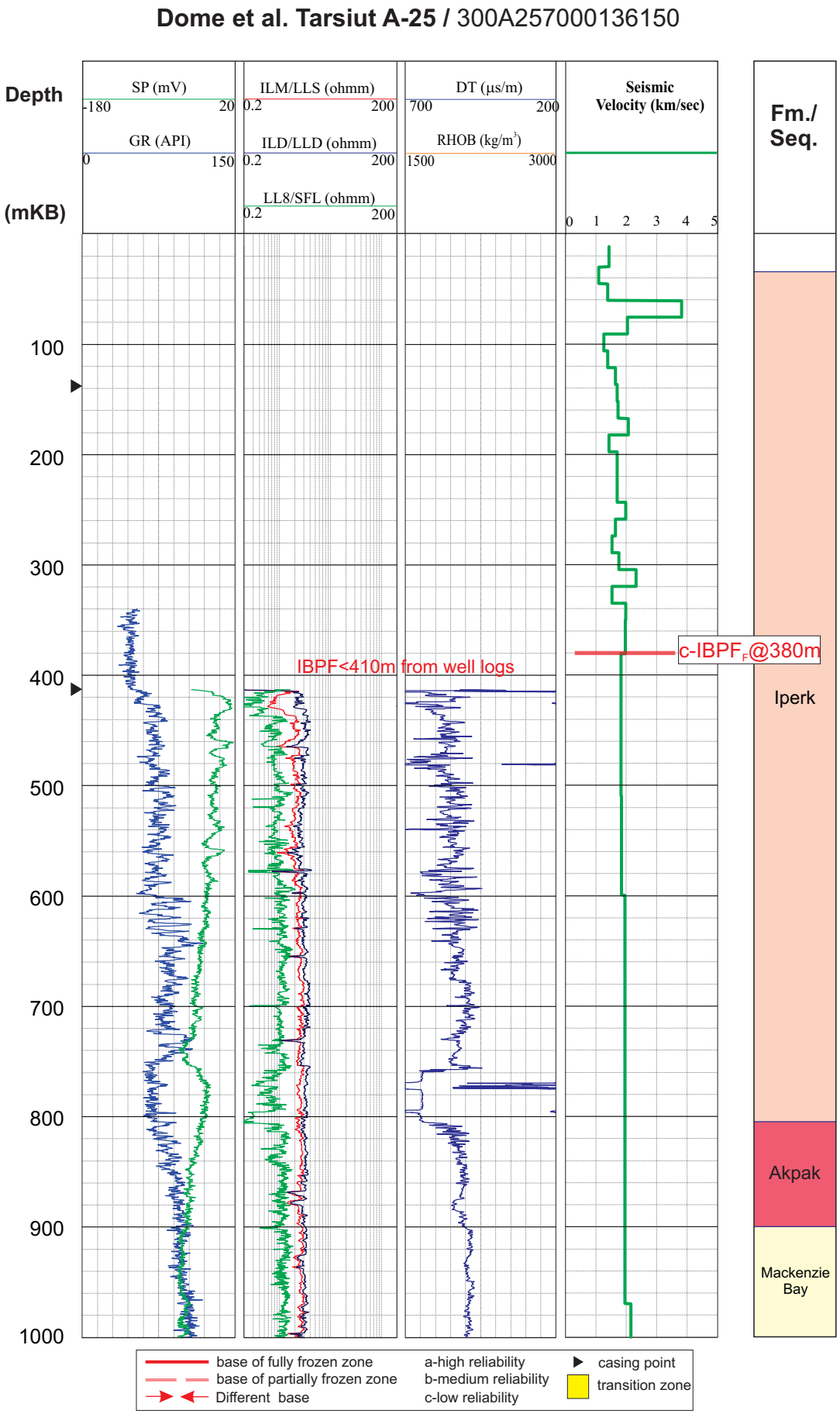

Figure 198. The base of permafrost is estimated from well seismic survey for the Tarsiut A-25 well in the Beaufort-Mackenzie Basin.

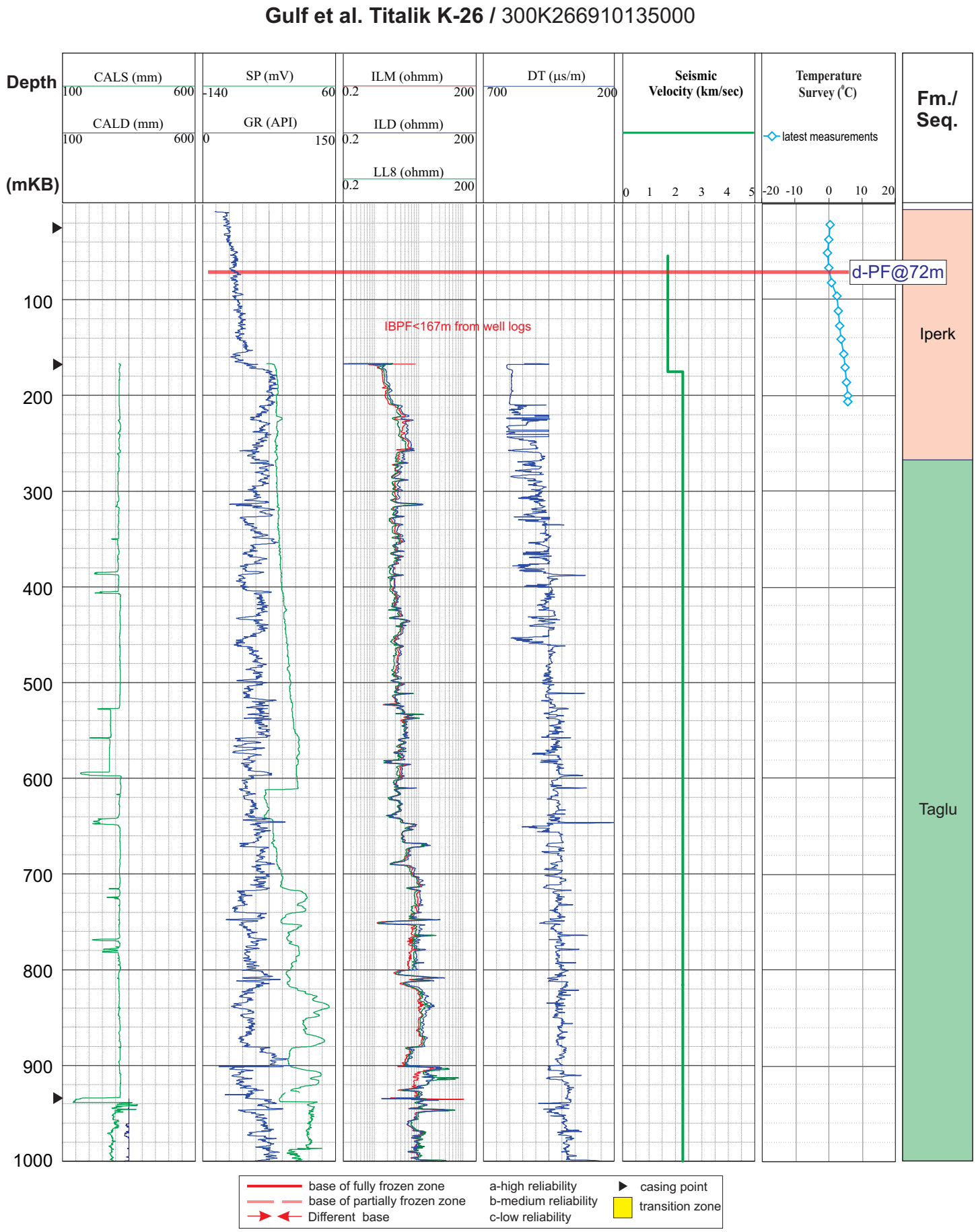

Figure 199. Determination of base of permafrost using temperature survey for the Titalik K-26 well in the Beaufort-Mackenzie Basin.

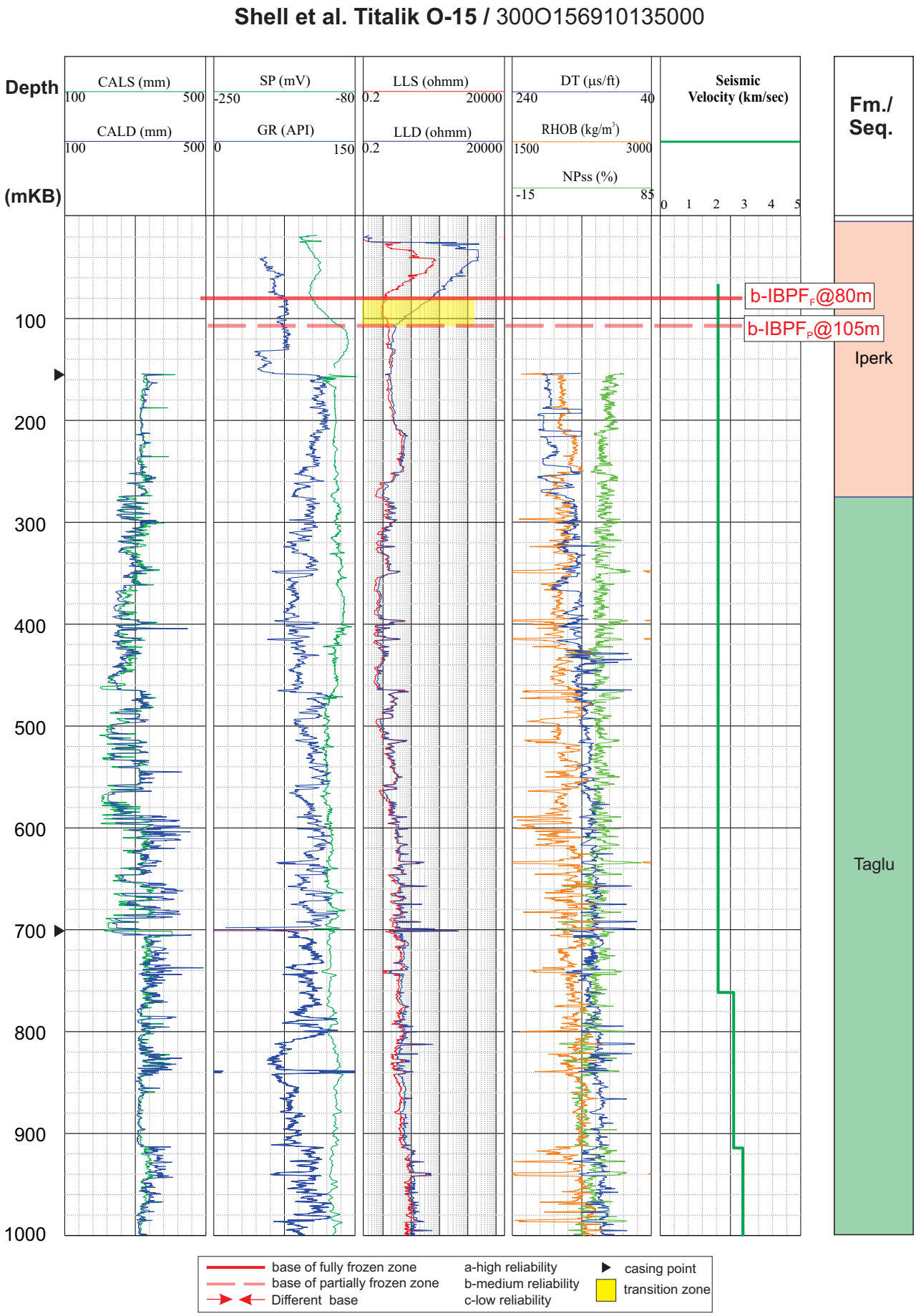

Figure 200. Determination of base of permafrost using well seismic survey and geophysical logs for the Titalik O-15 well in the Beaufort-Mackenzie Basin.

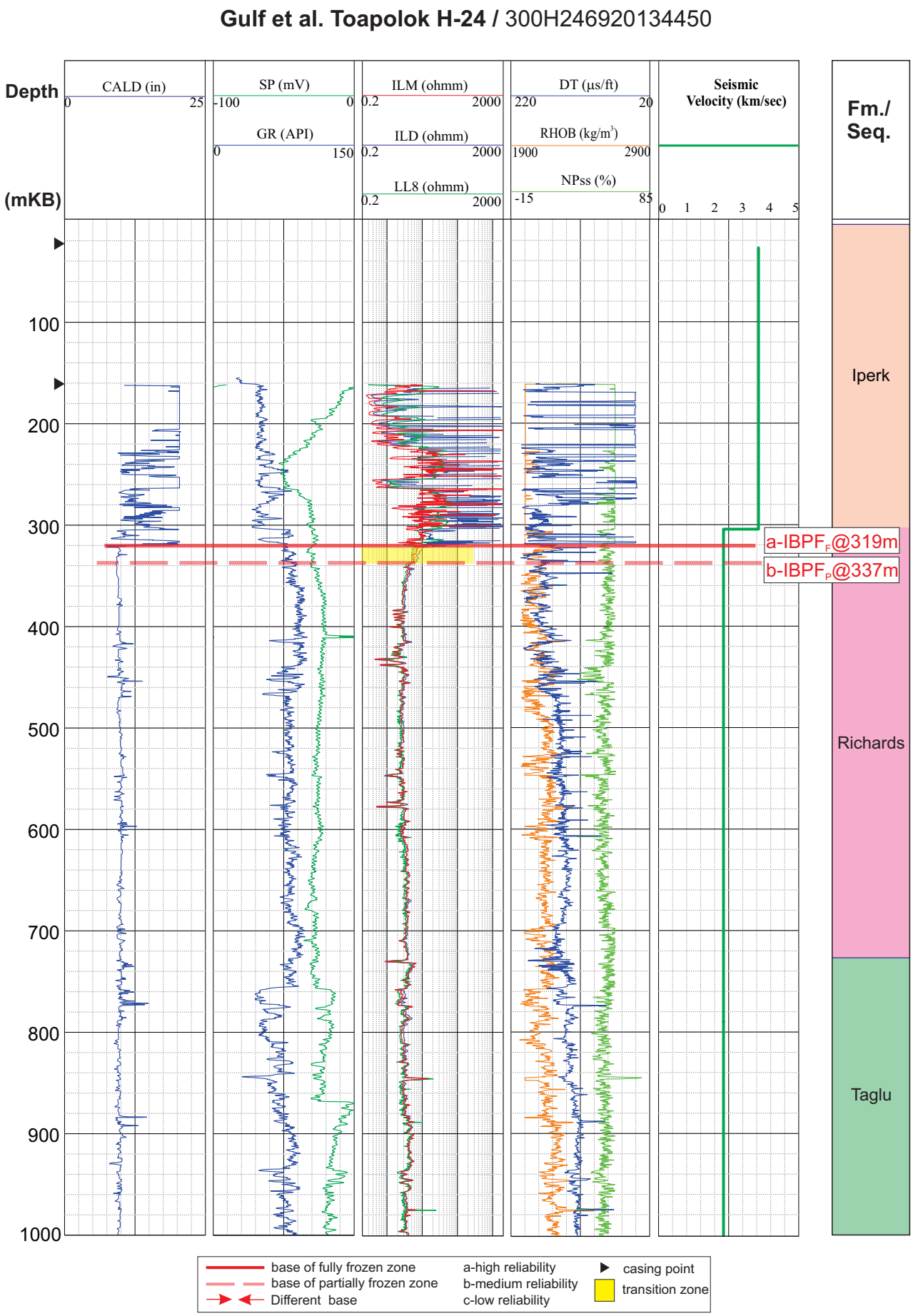

Figure 201. Determination of base of permafrost using well seismic survey and geophysical logs for the Toapolok H-24 well in the Beaufort-Mackenzie Basin.

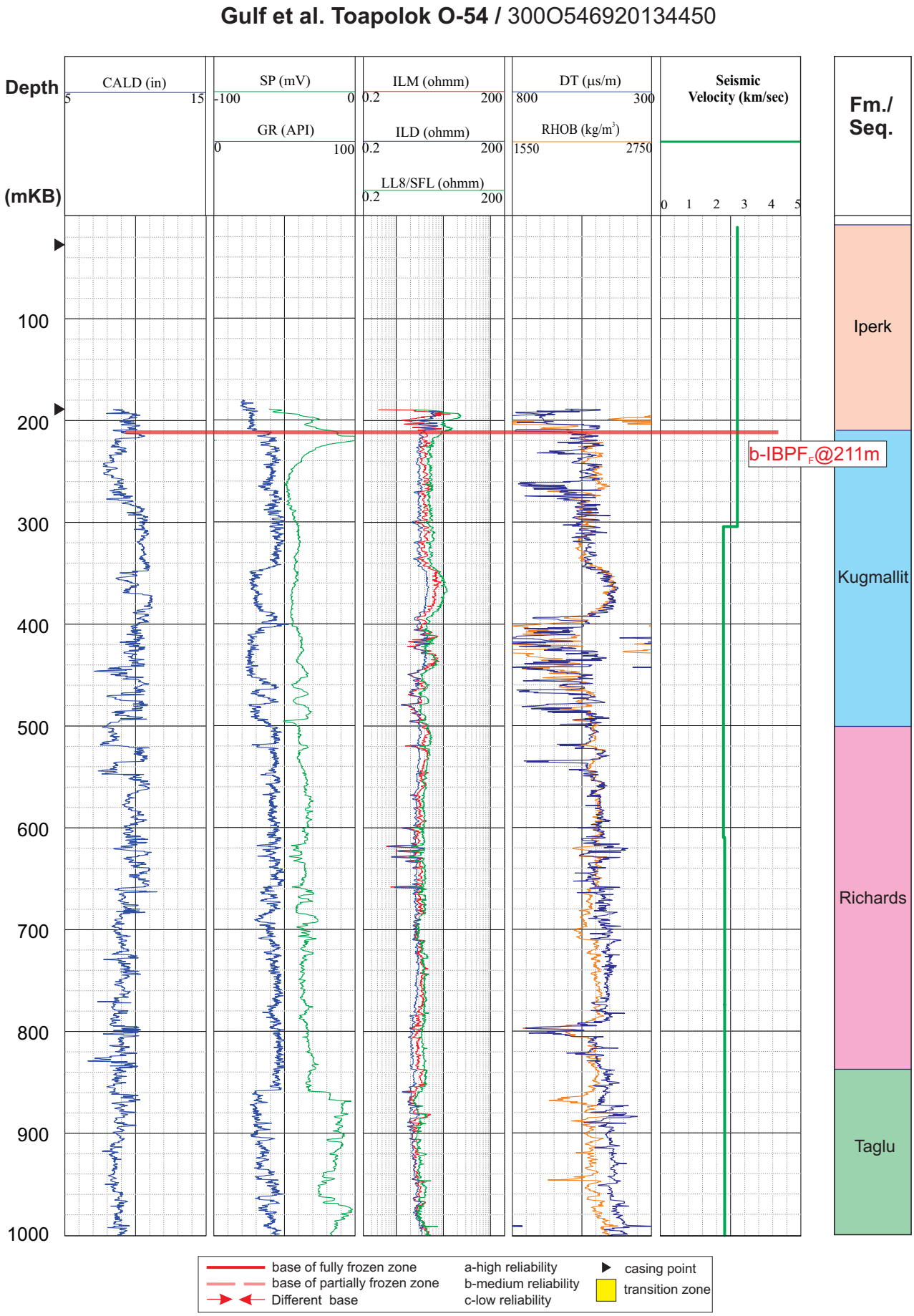

Figure 202. Determination of base of permafrost using well seismic survey and geophysical logs for the Toapolok O-54 well in the Beaufort-Mackenzie Basin.

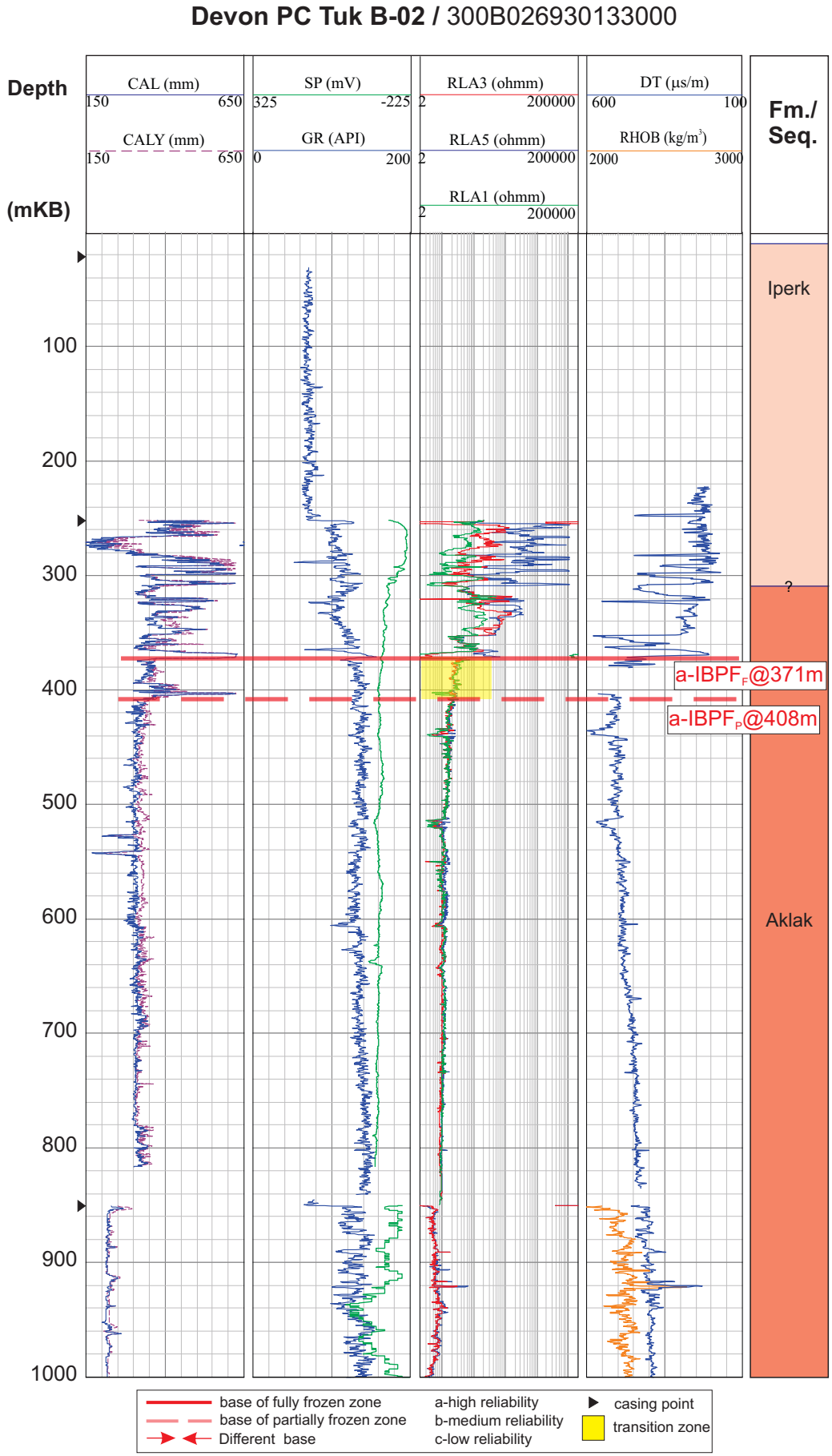

Figure 203. Determination of base of permafrost using geophysical logs for the Tuk B-02 well

Esso et al. Tuk B-40 / 300B406920133000

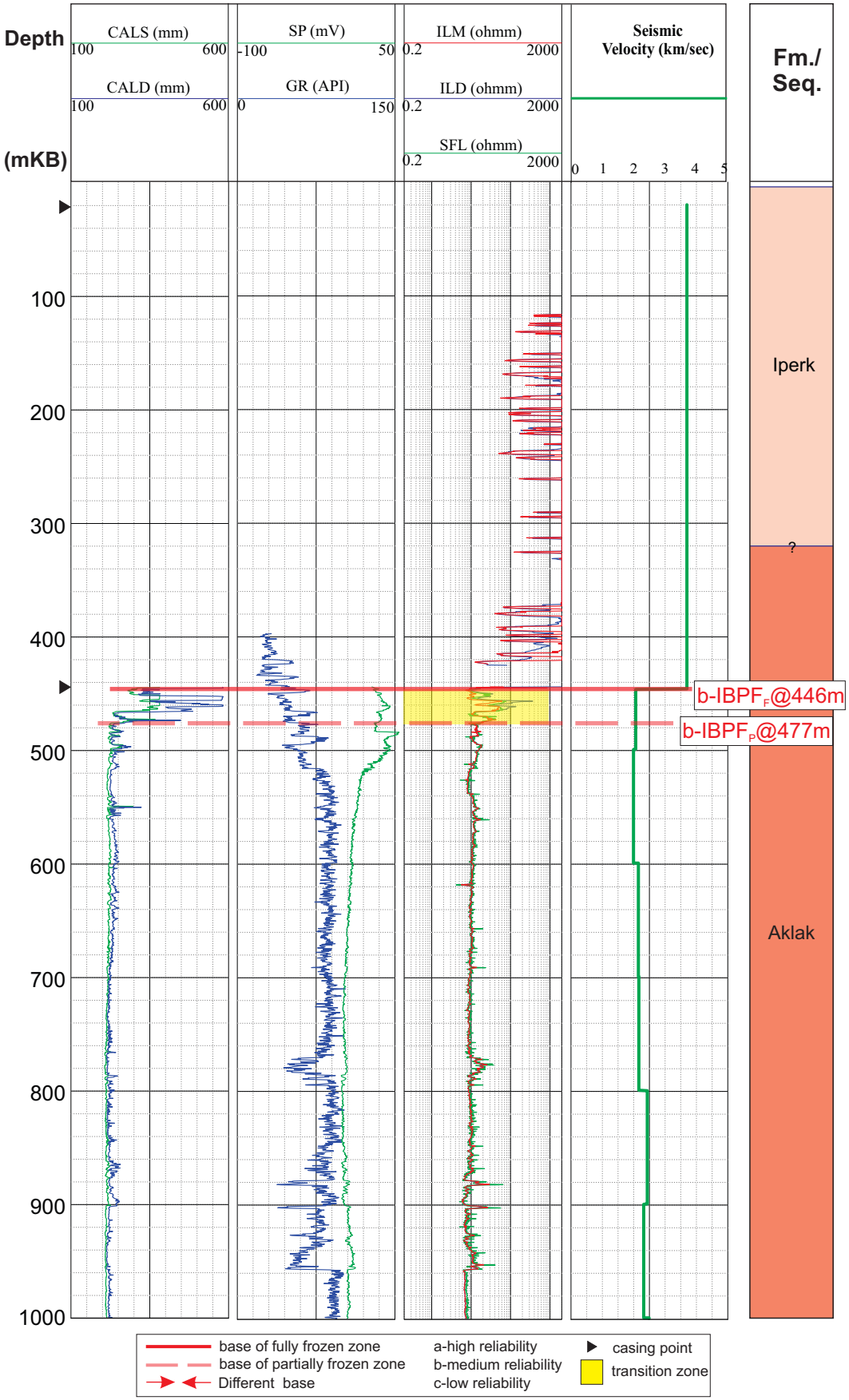

Figure 204. Determination of base of permafrost using well seismic survey and geophysical logs for the Tuk B-40 well in the Beaufort-Mackenzie Basin.

Esso et al. Tuk E-20 / 300E206920133000

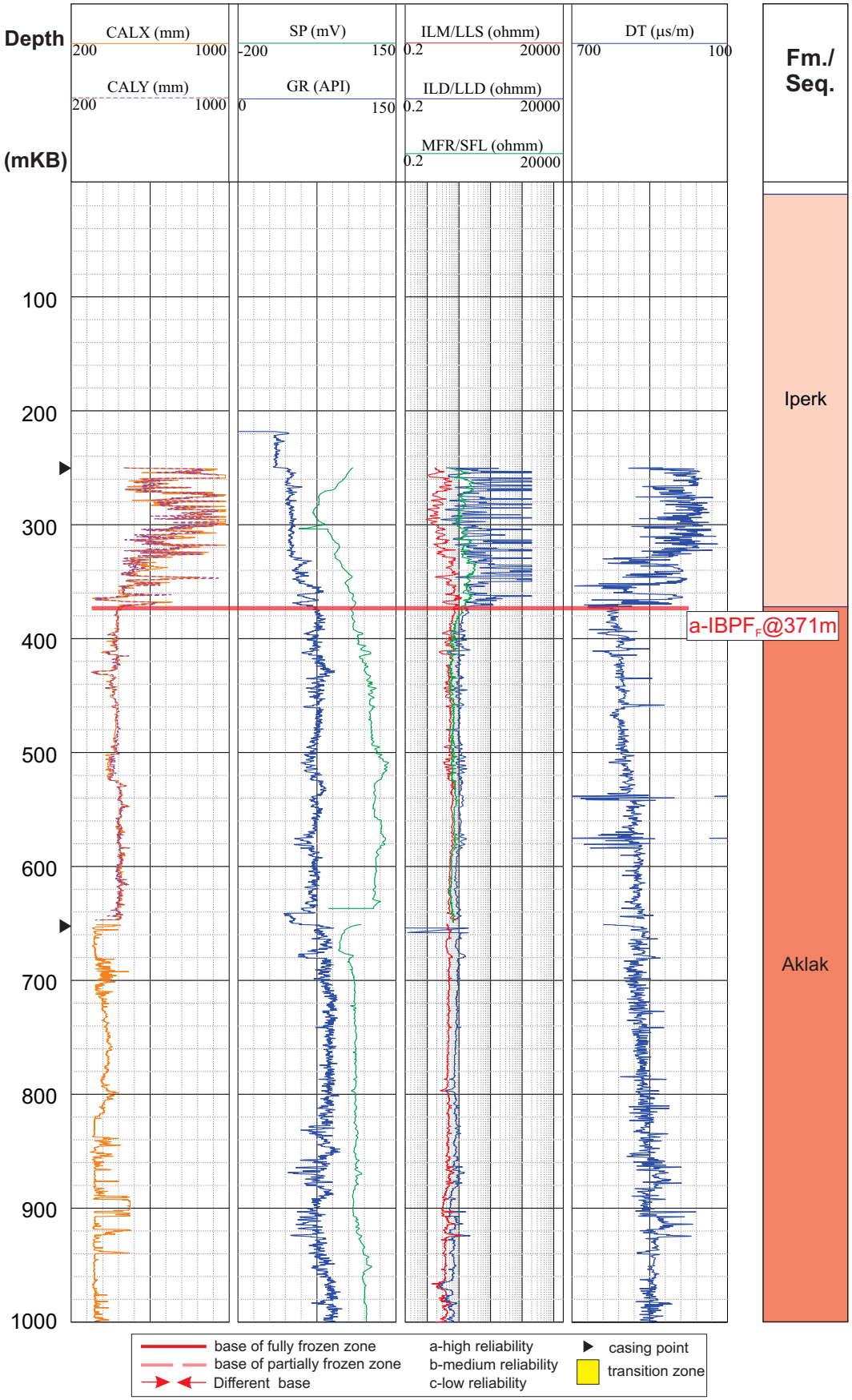

Figure 205. Determination of base of permafrost using geophysical logs for the Tuk E-20 well in the Beaufort-Mackenzie Basin.

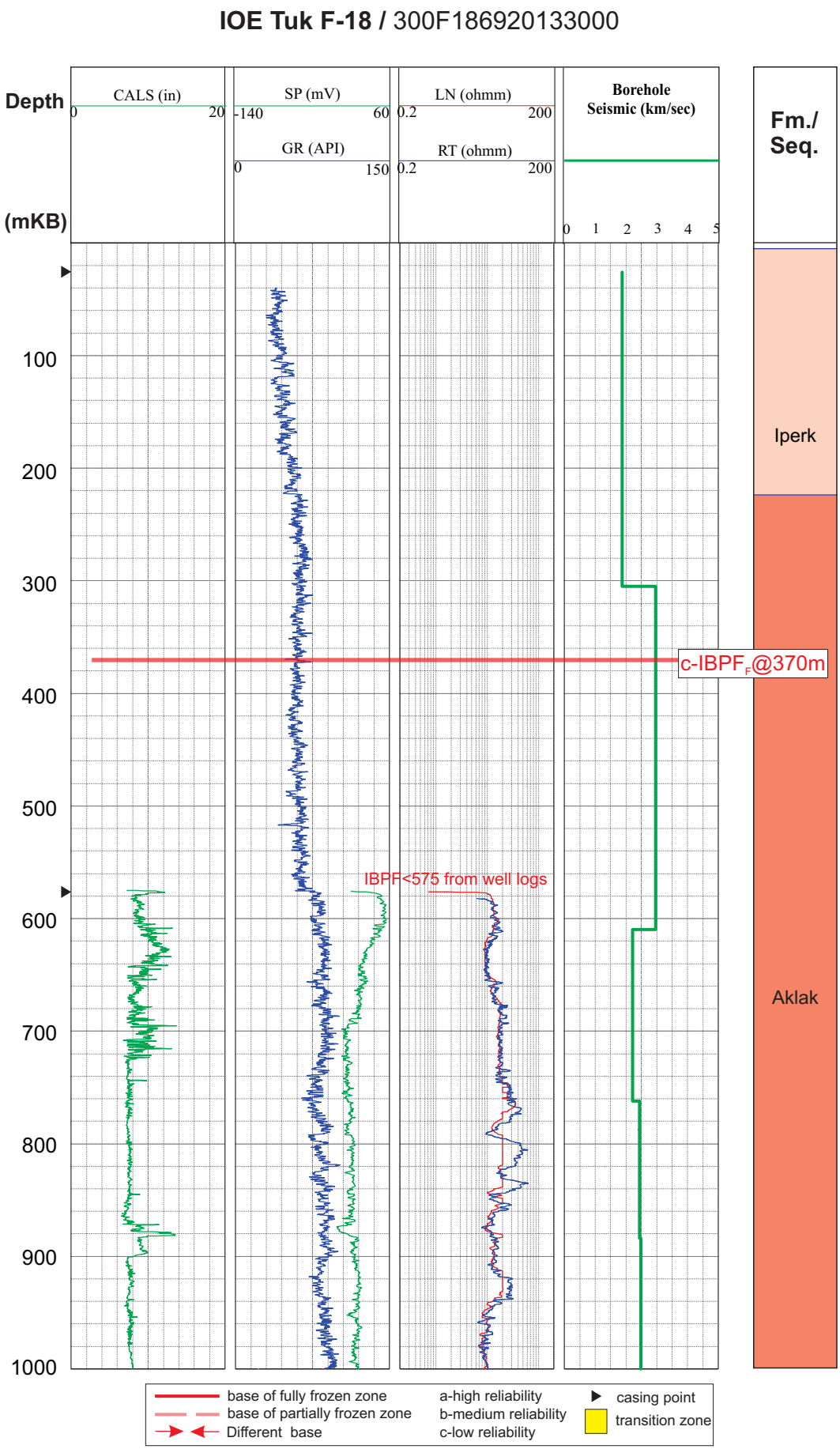

Figure 206. The base of permafrost is estimated mainly from well seismic survey, considering IBPF data of neighbor wells for the Tuk F-18 well in the Beaufort-Mackenzie Basin.

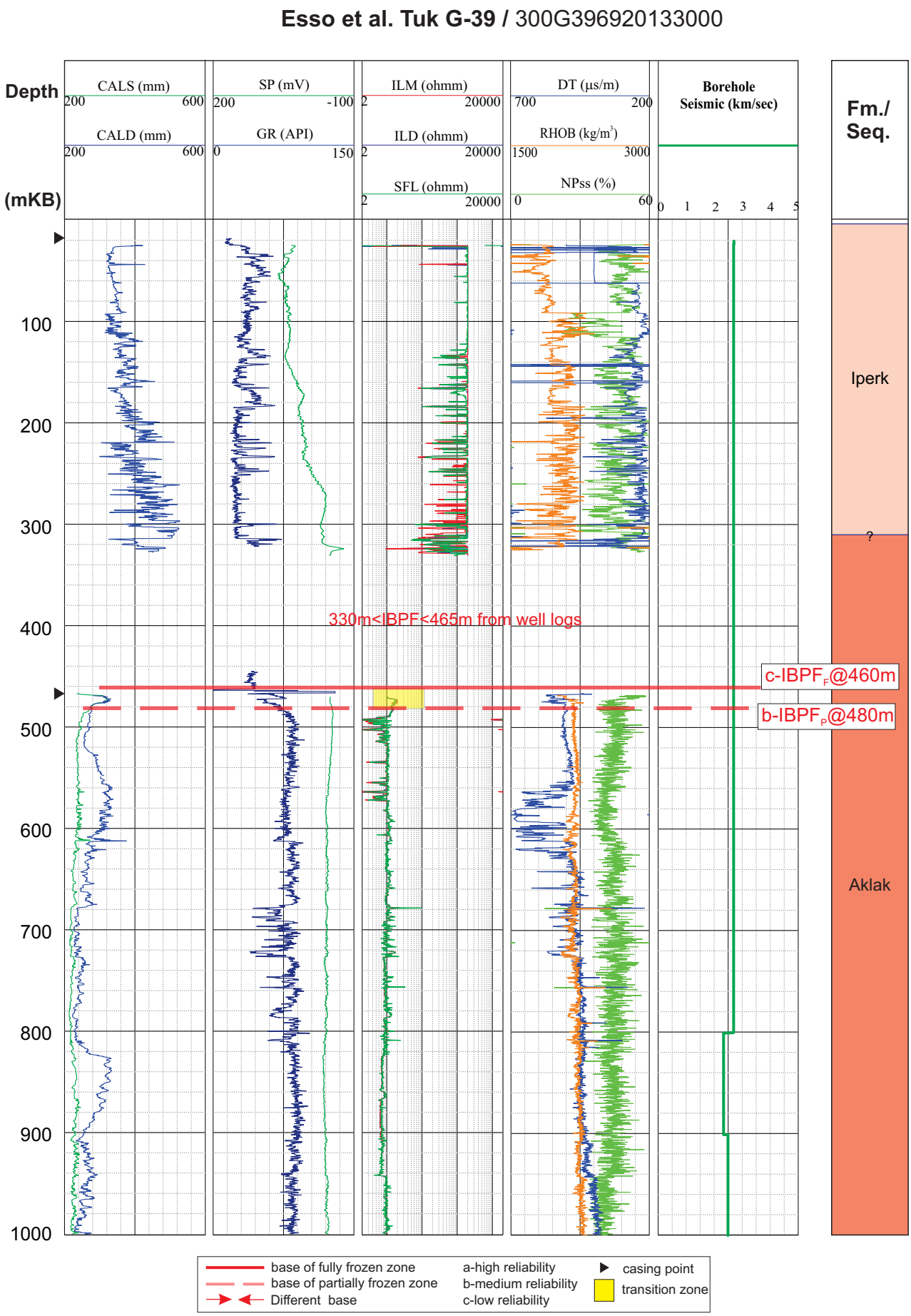

Figure 207. Determination of base of permafrost using well seismic survey and geophysical logs for the Tuk G-39 well in the Beaufort-Mackenzie Basin.

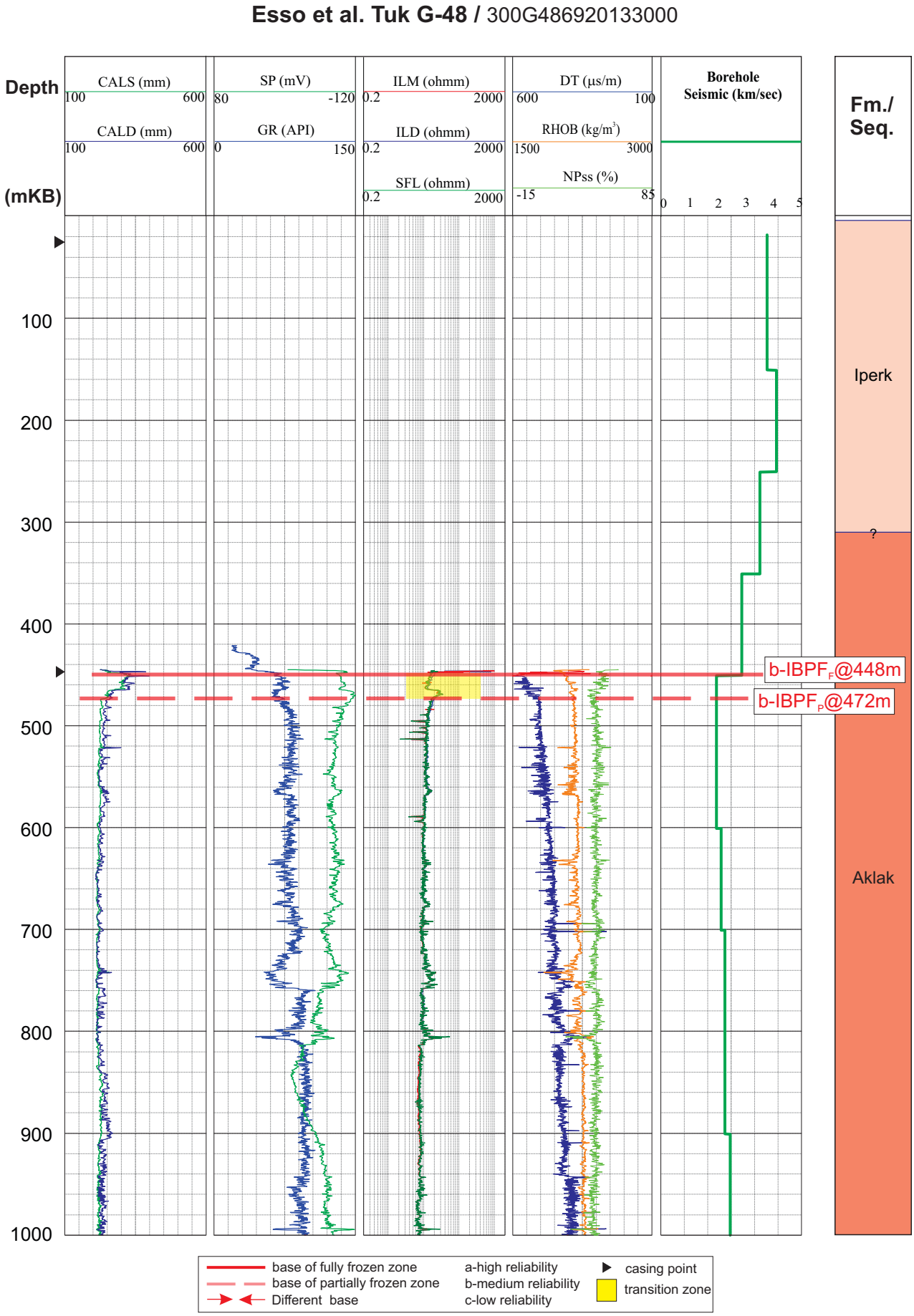

Figure 208. Determination of base of permafrost using well seismic survey and geophysical logs for the Tuk G-48 well in the Beaufort-Mackenzie Basin.

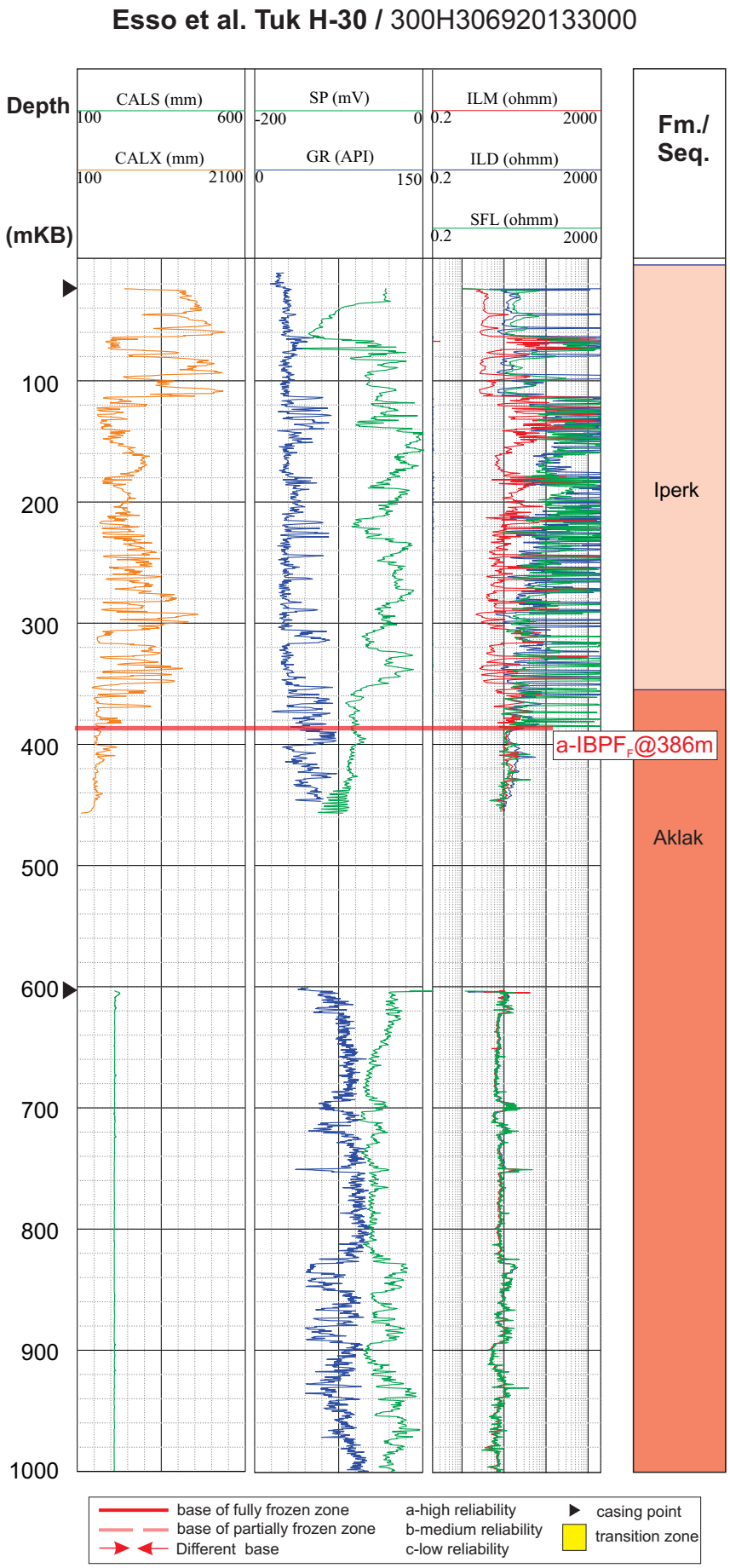

Figure 209. Determination of base of permafrost using geophysical logs for the Tuk H-30 well in the Beaufort-Mackenzie Basin.

Esso et al. Tuk J-29 / 300J296920133000

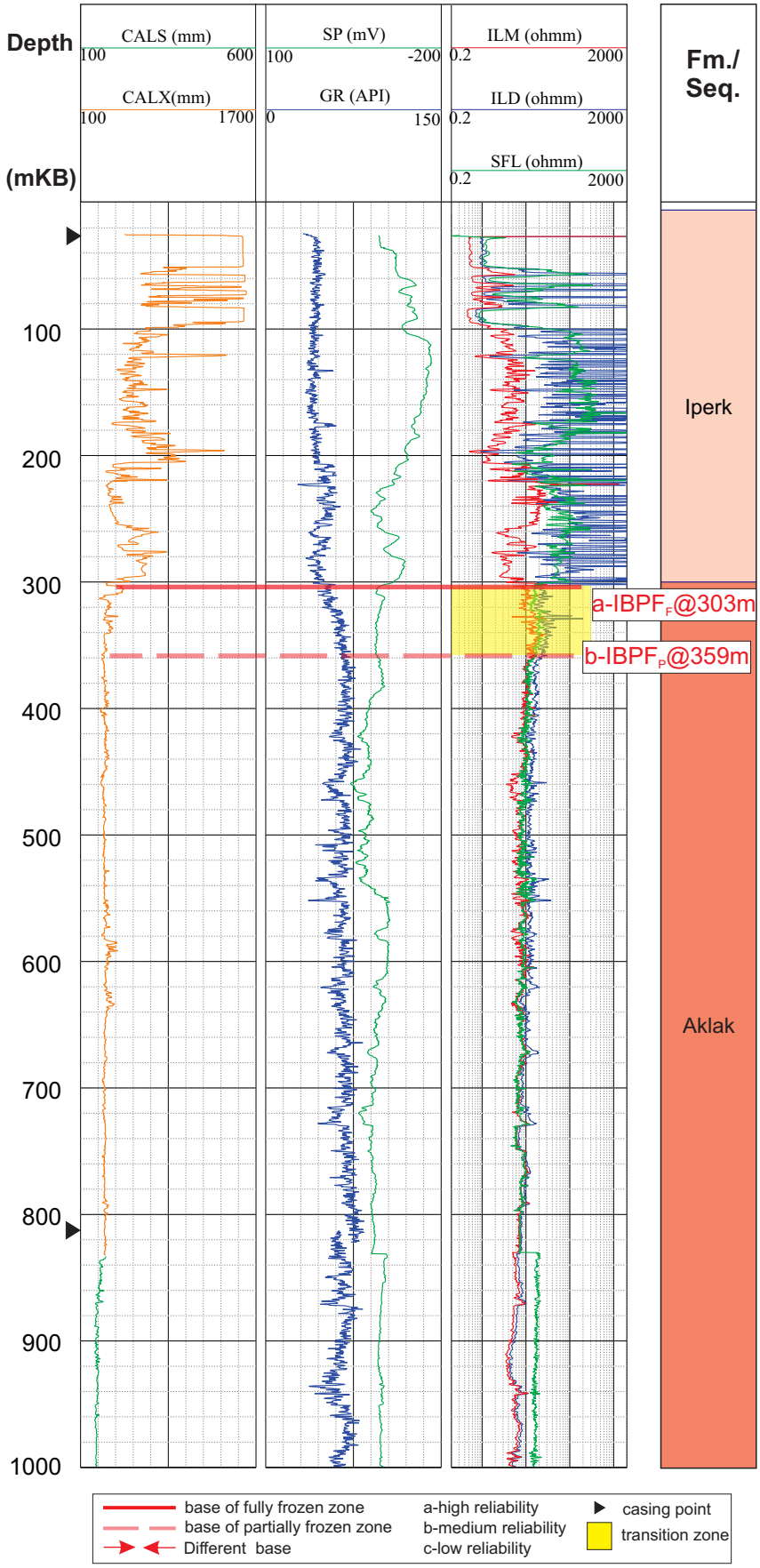

Figure 210. Determination of base of permafrost using geophysical logs for the Tuk J-29 well in the Beaufort-Mackenzie Basin.

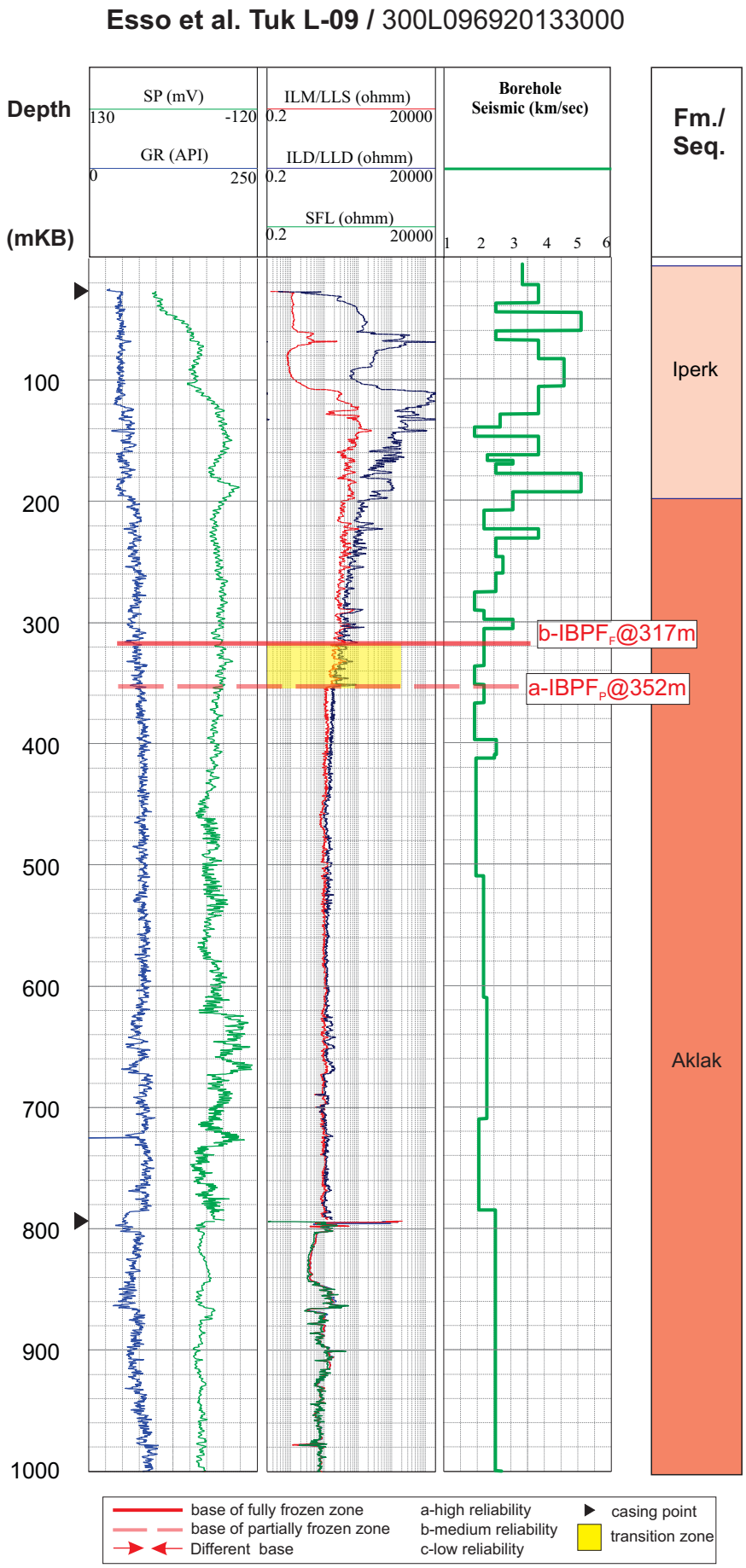

Figure 211. Determination of base of permafrost using well seismic survey and geophysical logs for the Tuk L-09 (M-09) well in the Beaufort-Mackenzie Basin.

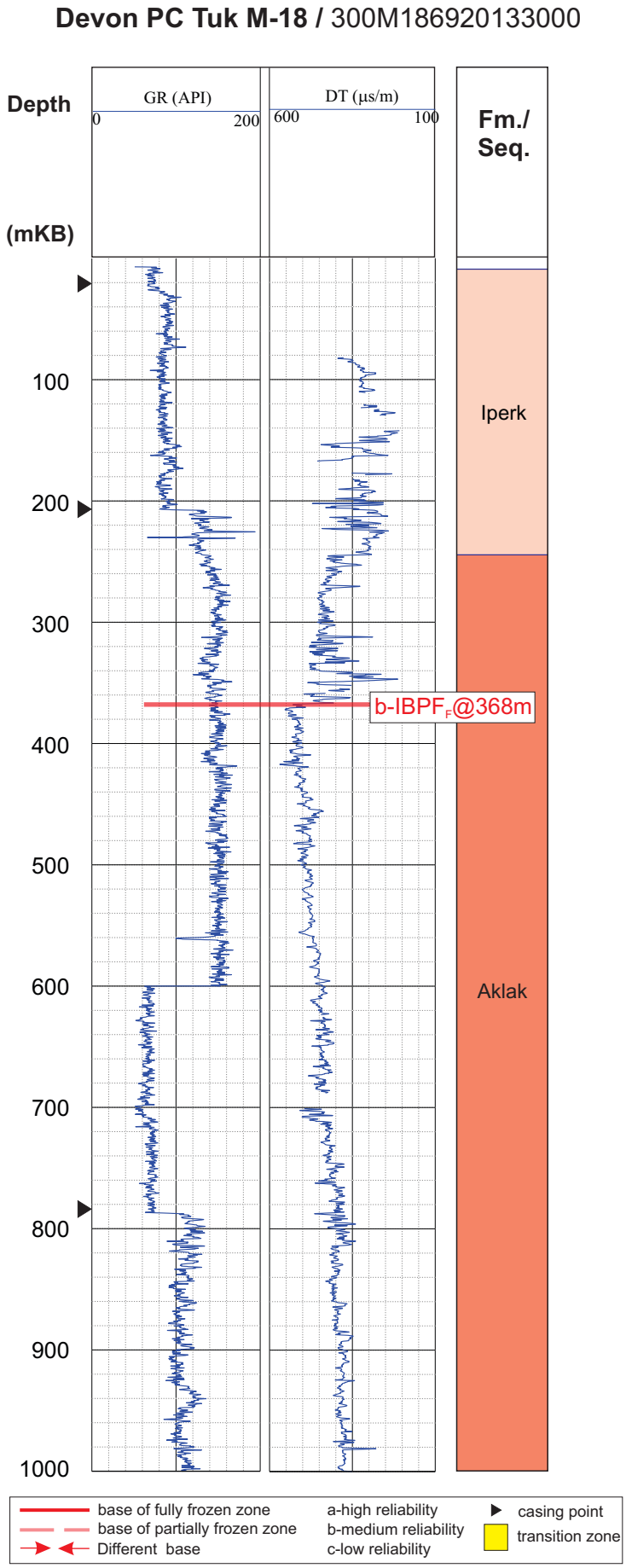

Figure 212. Determination of base of permafrost using geophysical logs for the Tuk M-18 well in the Beaufort-Mackenzie Basin.

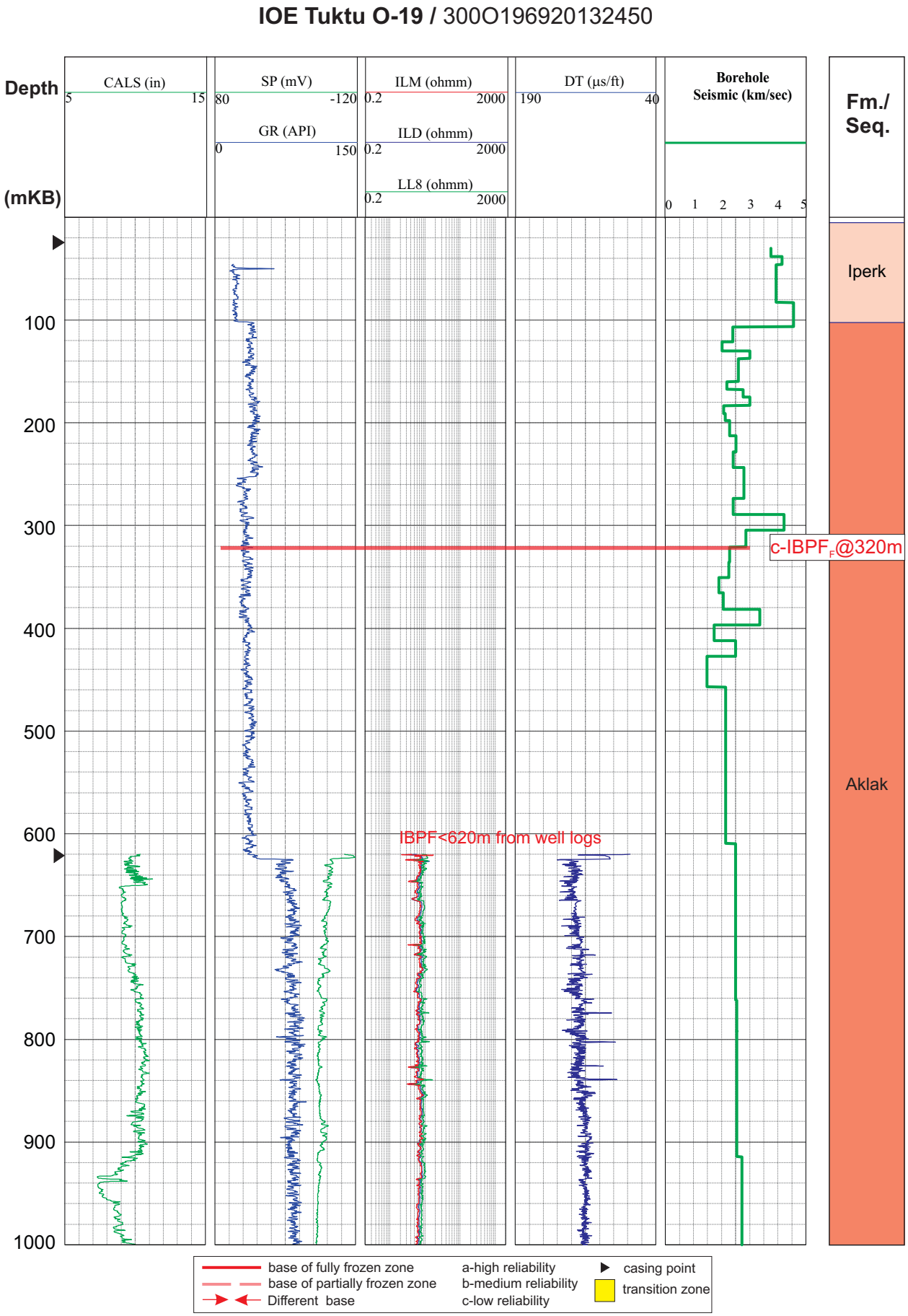

Figure 213. The base of permafrost is estimated from well seismic survey for the Tuktu O-19 well in the Beaufort-Mackenzie Basin.

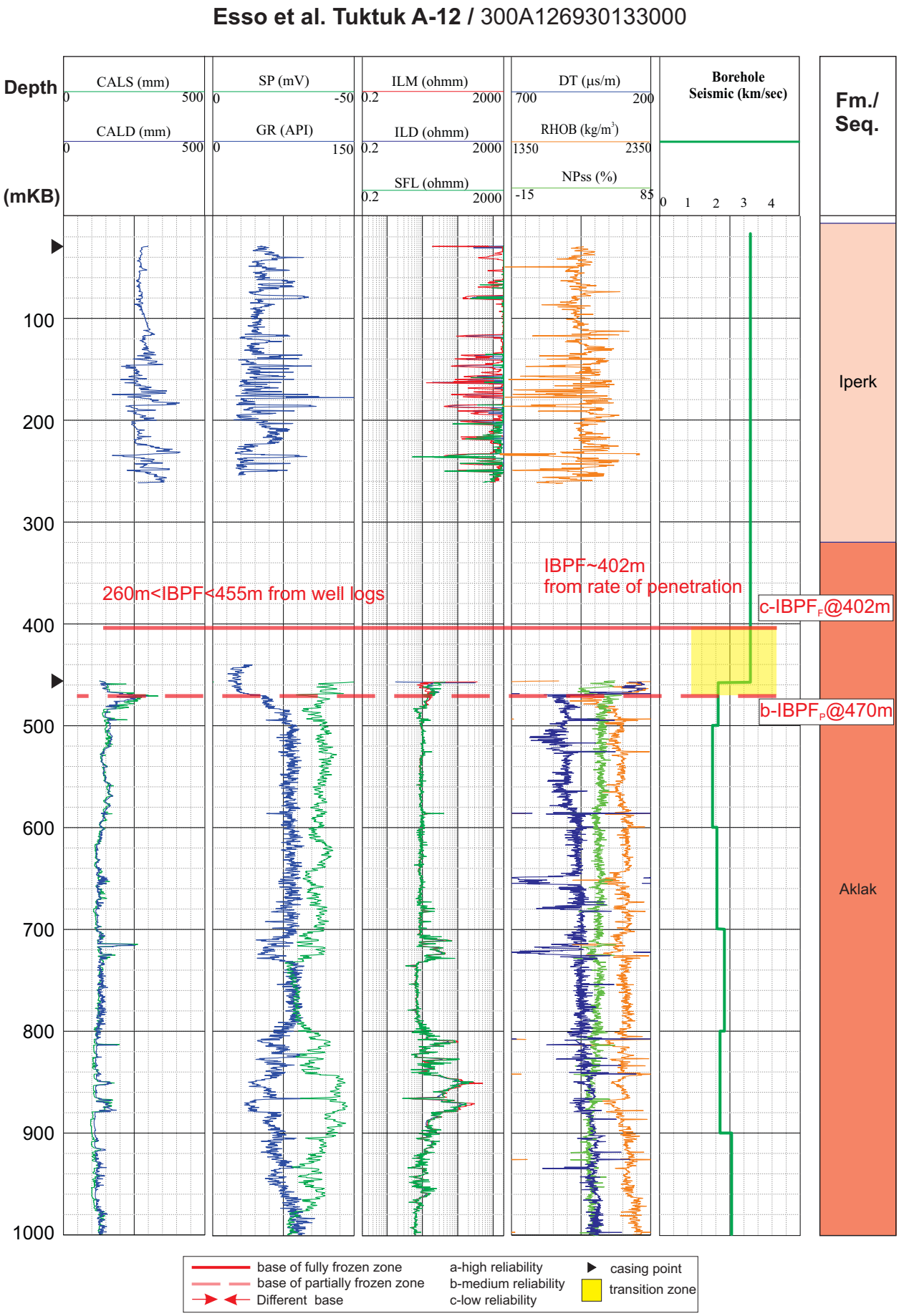

Figure 214. Determination of base of permafrost using well seismic survey and geophysical logs, as well as rate of penetration for the Tuktuk A-12 well in the Beaufort-Mackenzie Basin.

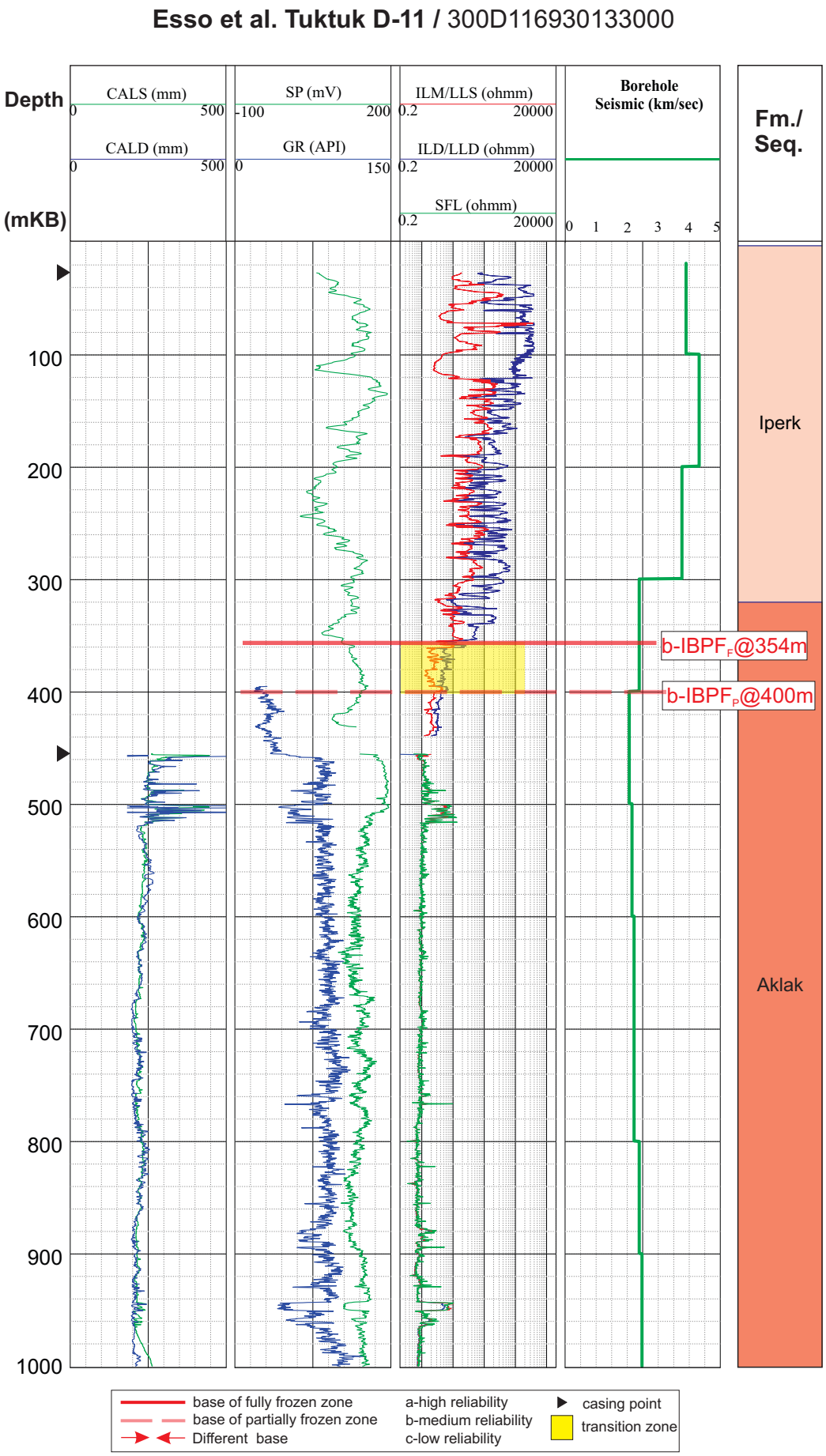

Figure 215. Determination of base of permafrost using well seismic survey and geophysical logs for the Tuktuk D-11 well in the Beaufort-Mackenzie Basin.

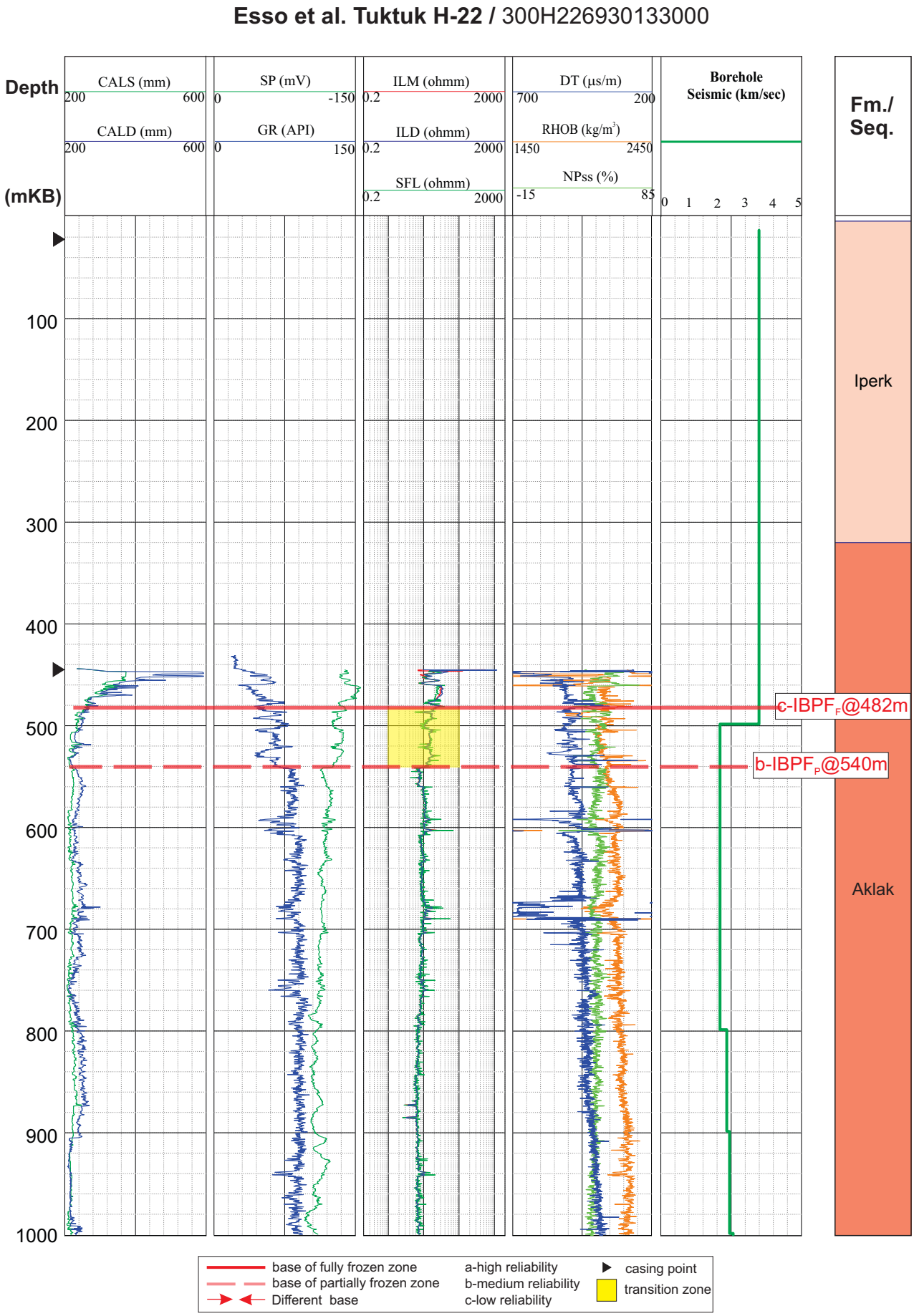

Figure 216. Determination of base of permafrost using well seismic survey and geophysical logs for the Tuktuk H-22 well in the Beaufort-Mackenzie Basin.

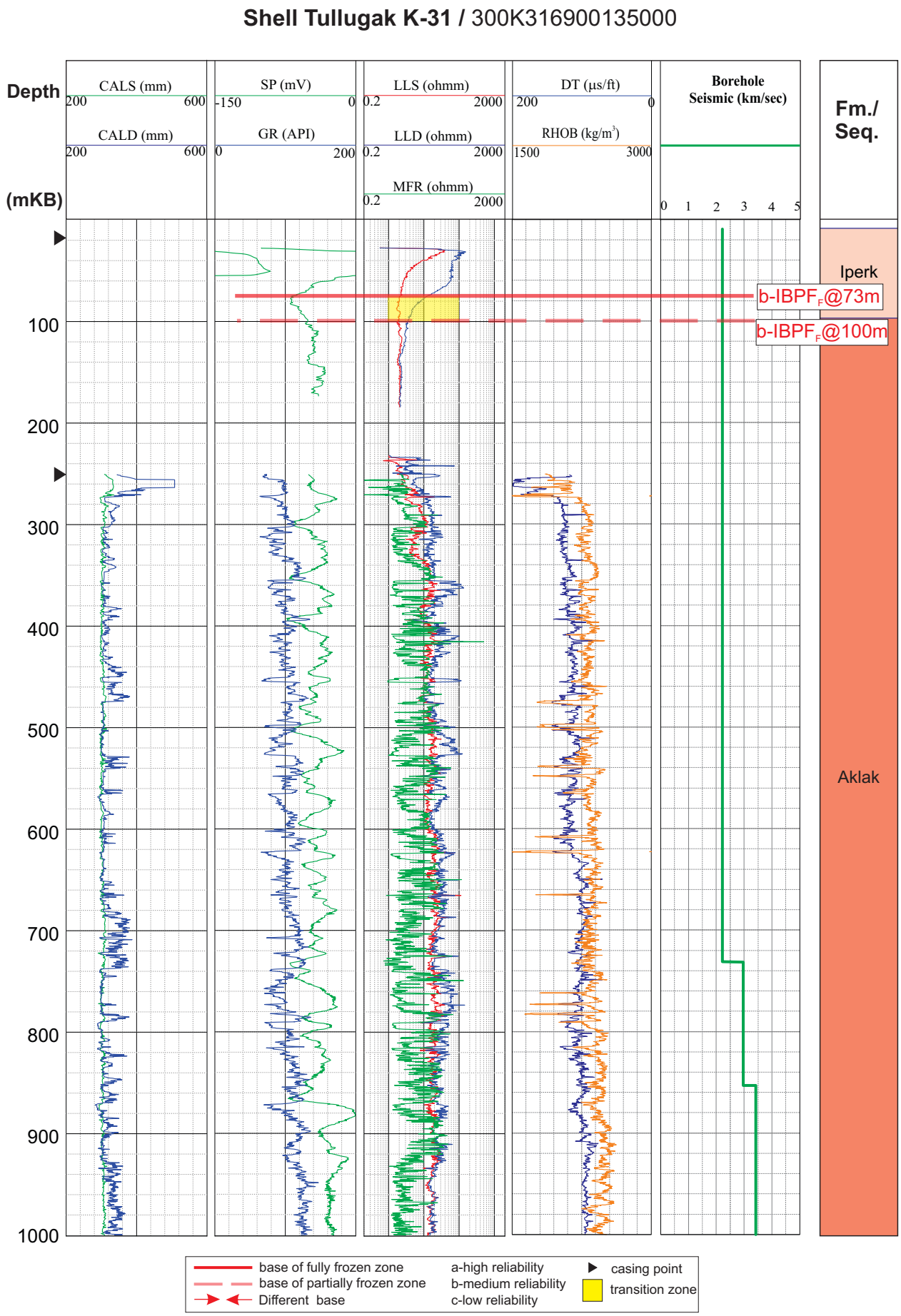

Figure 217. Determination of base of permafrost using well seismic survey and geophysical logs for the Tullugak K-31 well in the Beaufort-Mackenzie Basin.

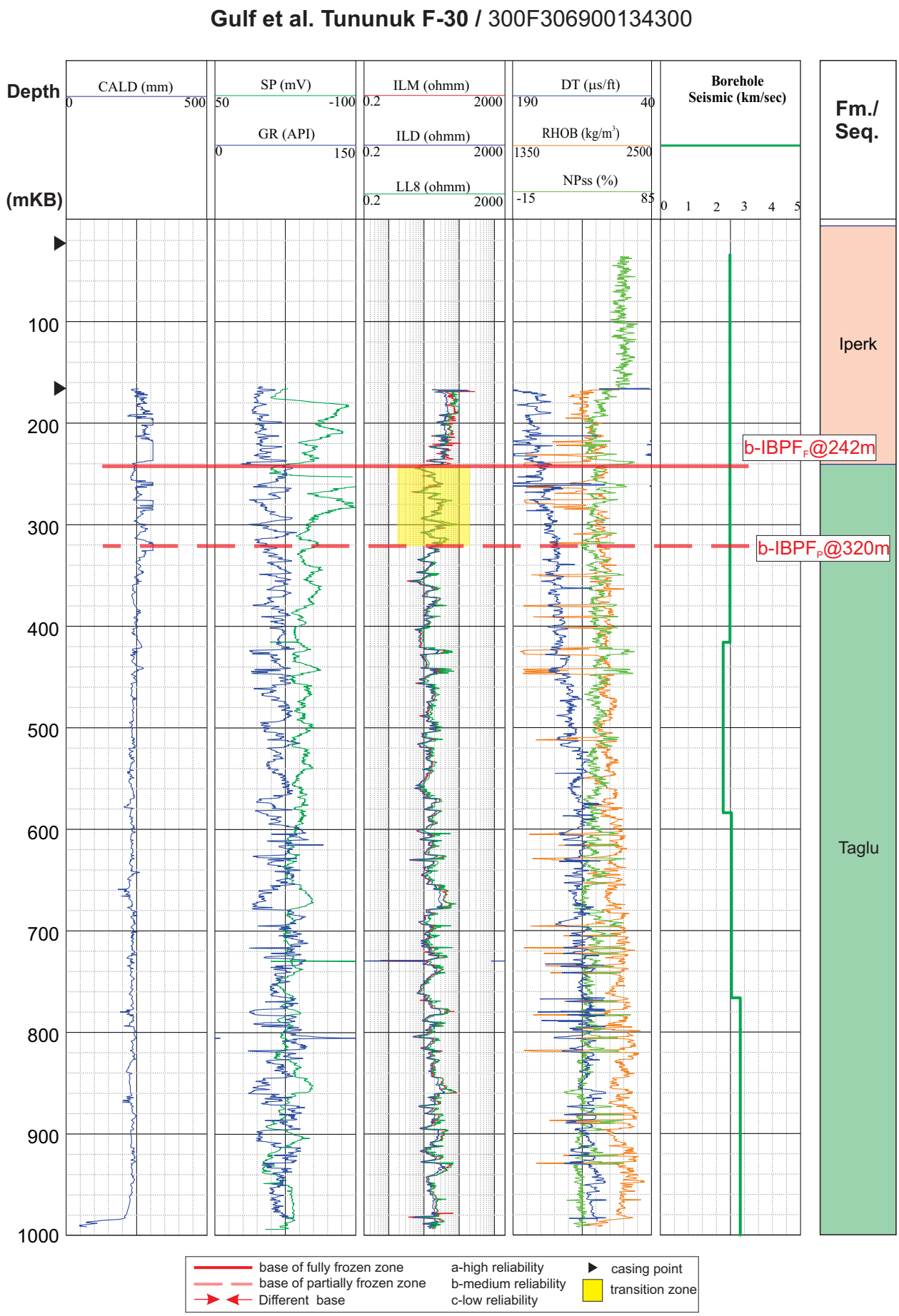

Figure 218. Determination of base of permafrost using well seismic survey and geophysical logs for the Tununuk F-30 well in the Beaufort-Mackenzie Basin.

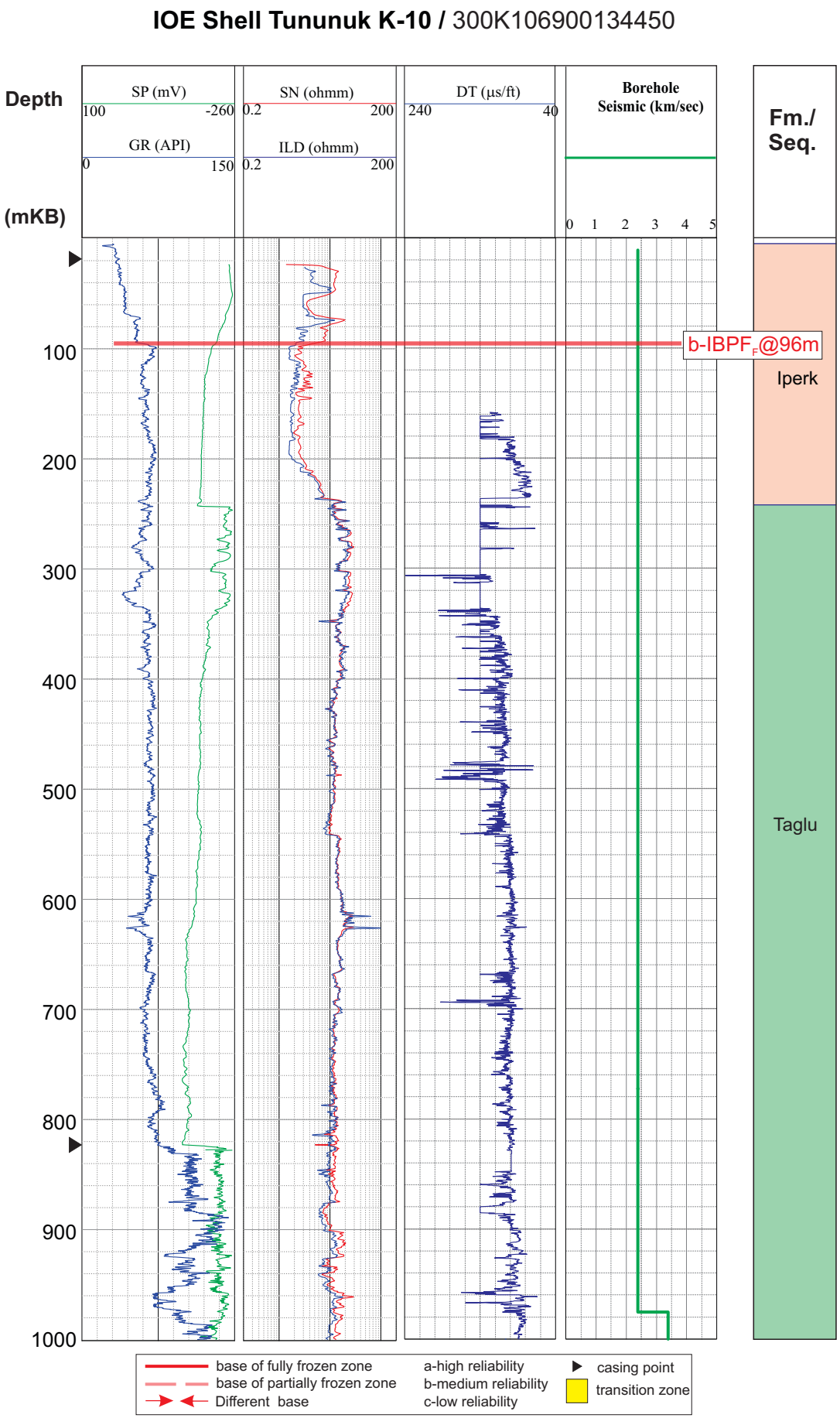

Figure 219. Determination of base of permafrost using well seismic survey and geophysical logs for the Tununuk K-10 well in the Beaufort-Mackenzie Basin.

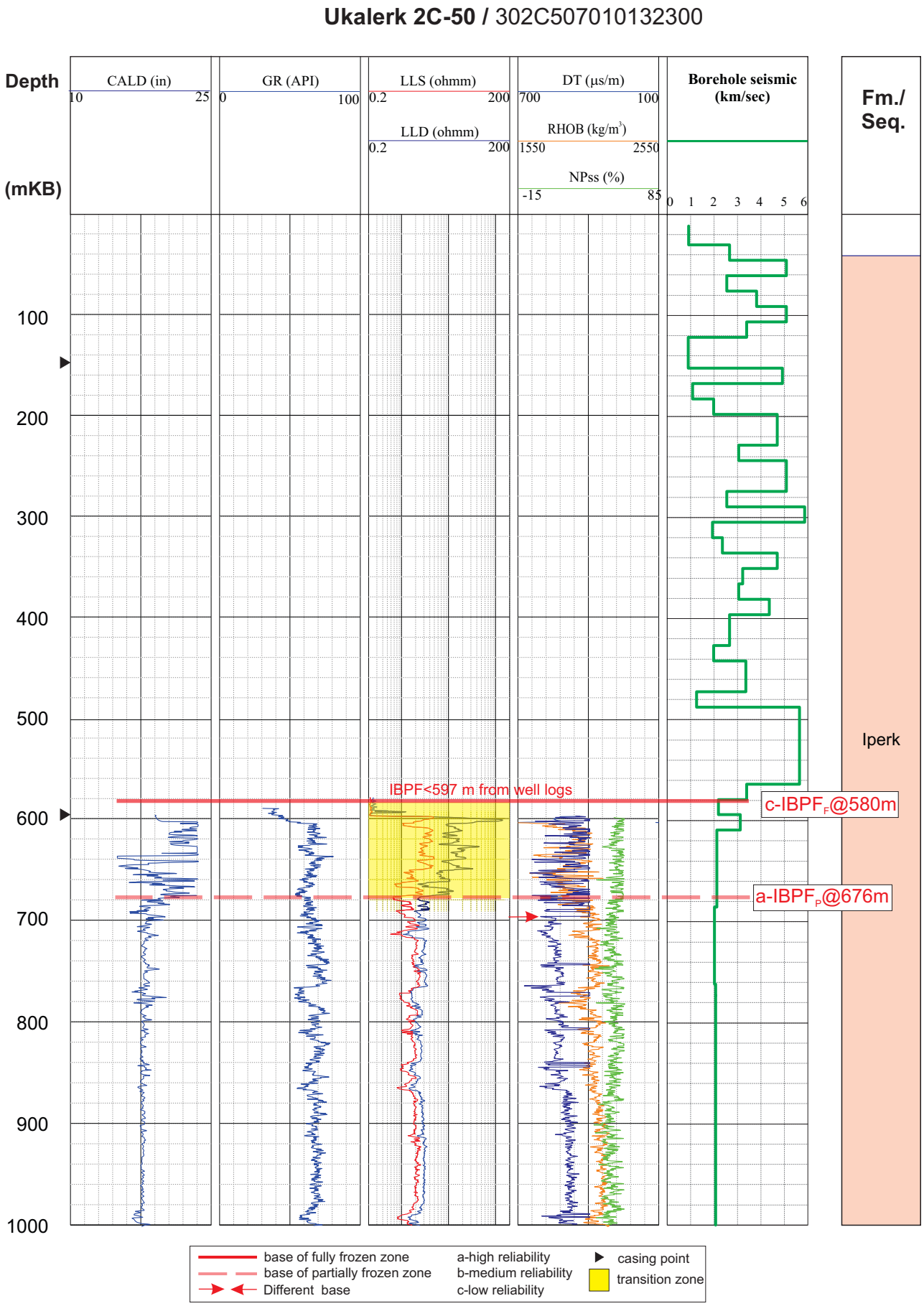

Figure 220. Determination of base of permafrost using well seismic survey and geophysical logs for the Ukalerk 2C-50 well in the Beaufort-Mackenzie Basin.

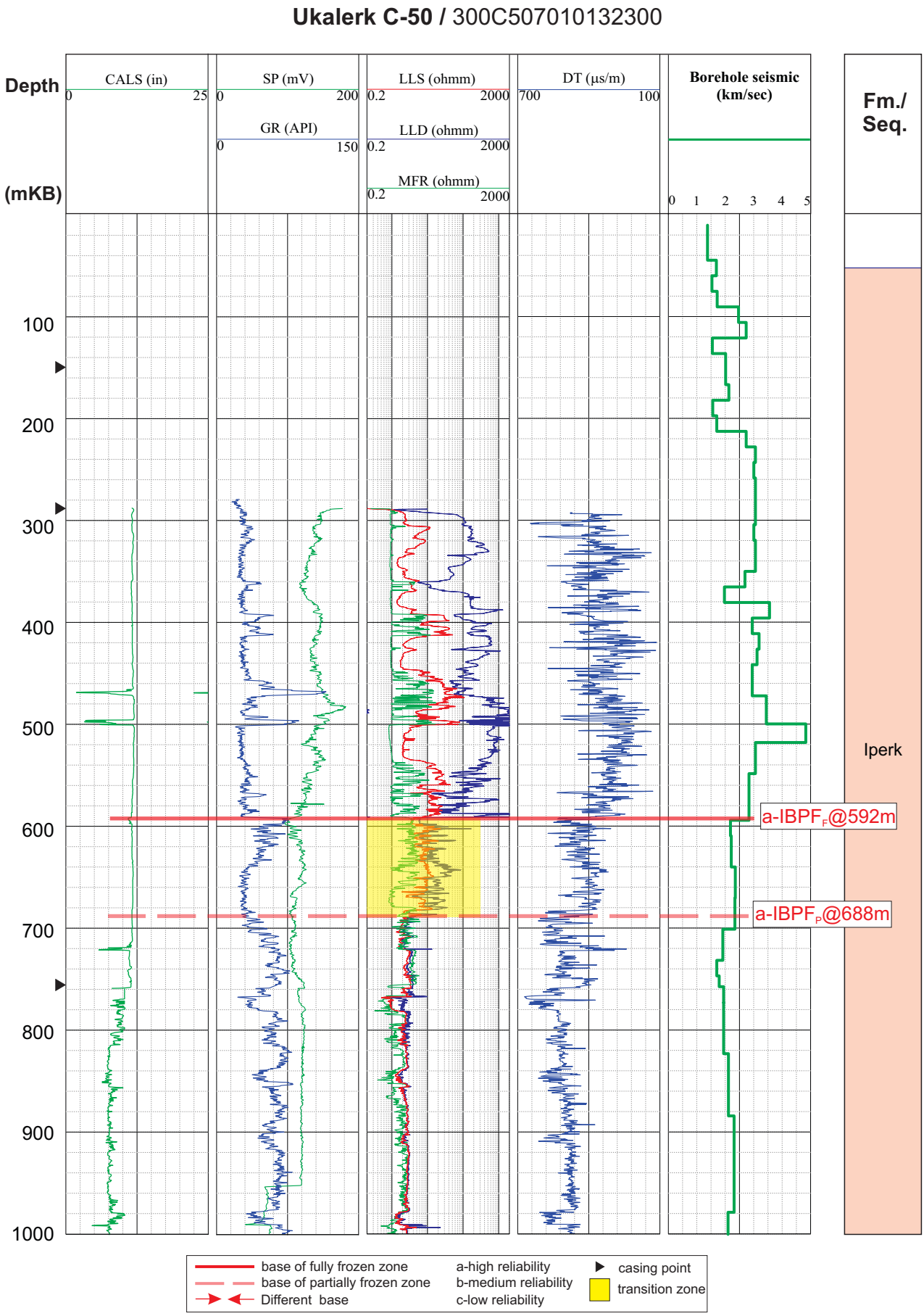

Figure 221. Determination of base of permafrost using well seismic survey and geophysical logs for the Ukalerk C-50 well in the Beaufort-Mackenzie Basin.

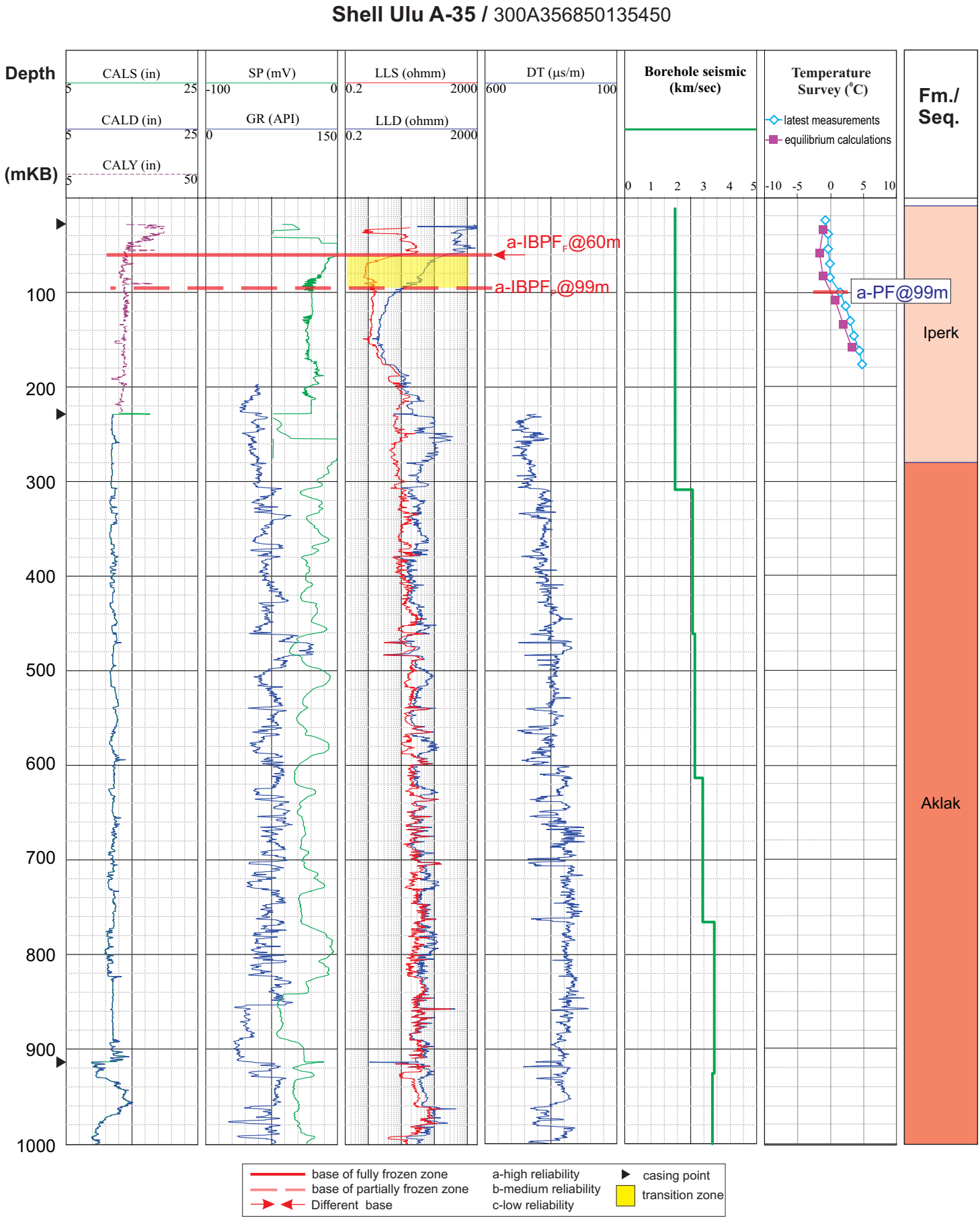

Figure 222. Determination of base of permafrost using temperature survey, well seismic survey and geophysical logs for the Ulu A-35 well in the Beaufort-Mackenzie Basin.

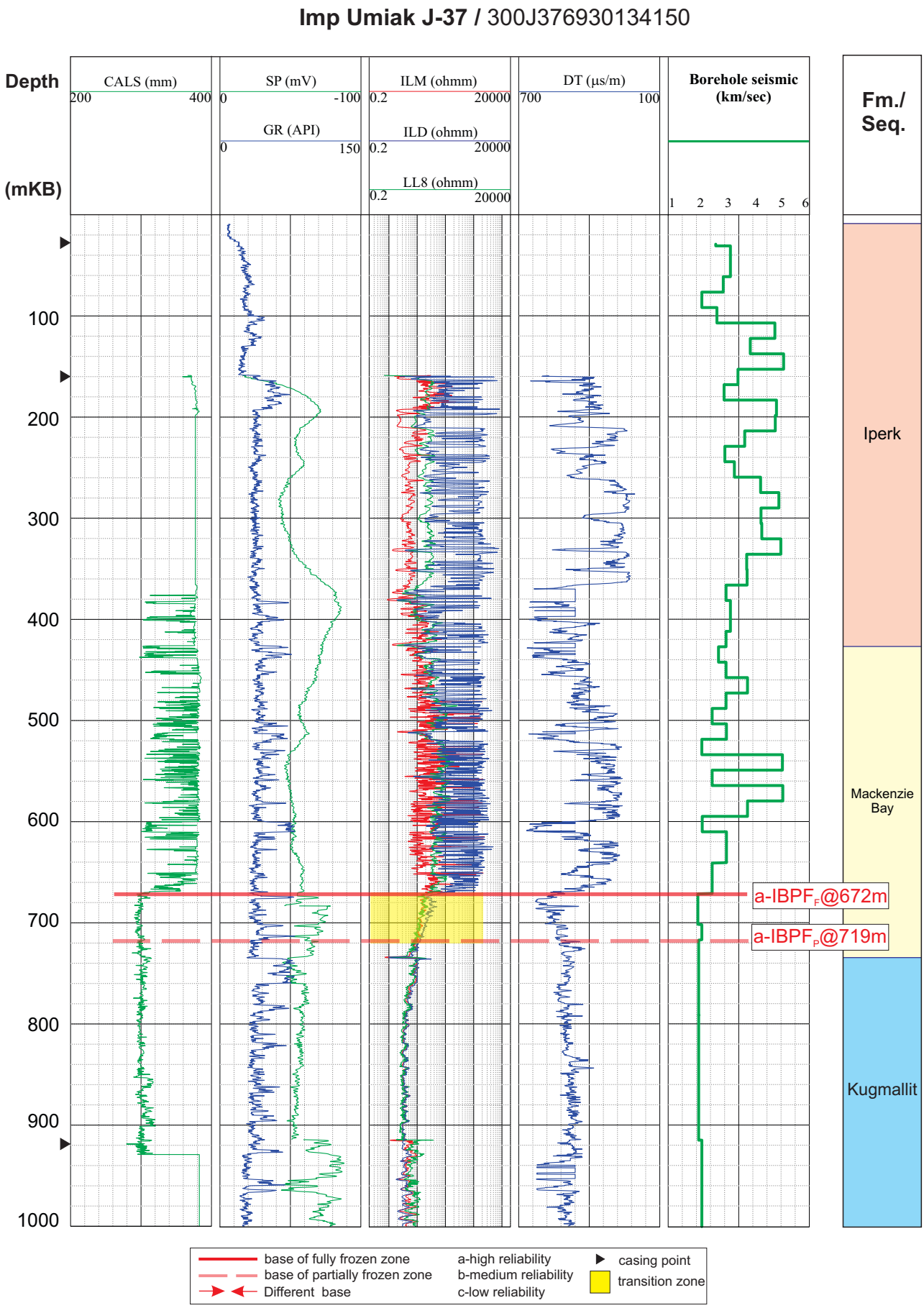

Figure 223. Determination of base of permafrost using well seismic survey and geophysical logs for the Umiak J-37 well in the Beaufort-Mackenzie Basin.

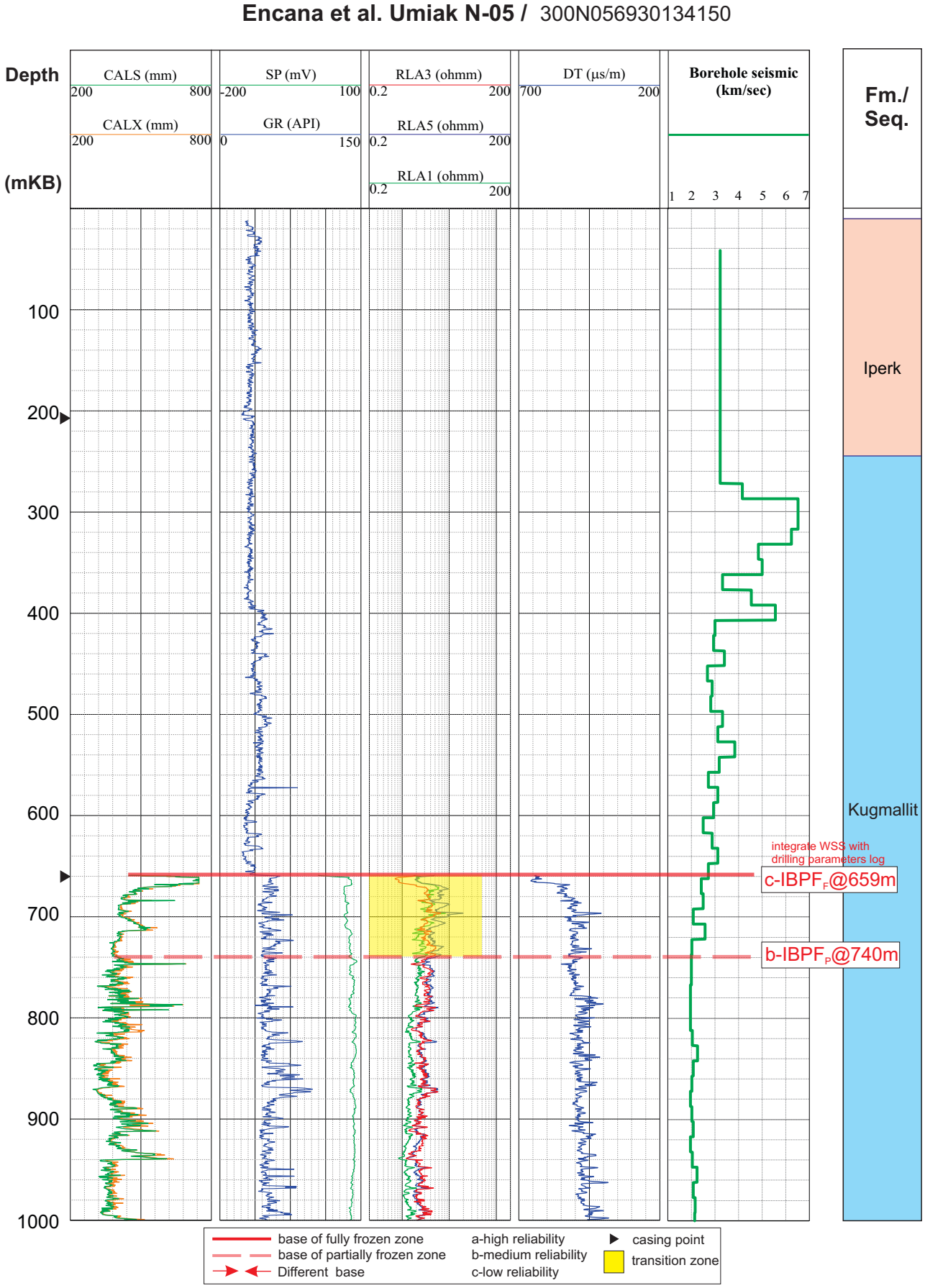

Figure 224. Log suite and borehole seismic survey data for the shallow interval of the Umiak N-05 well in the Beaufort-Mackenzie Basin, possible fully frozen base of permafrost is based on borehole seismic surveys, and drilling parameters log (including ROP-rate of penetration, inlet and outlet mud temperature while drilling, and WOB-weight on bit). The partially frozen base is from combination of well logs and seismic surveys.

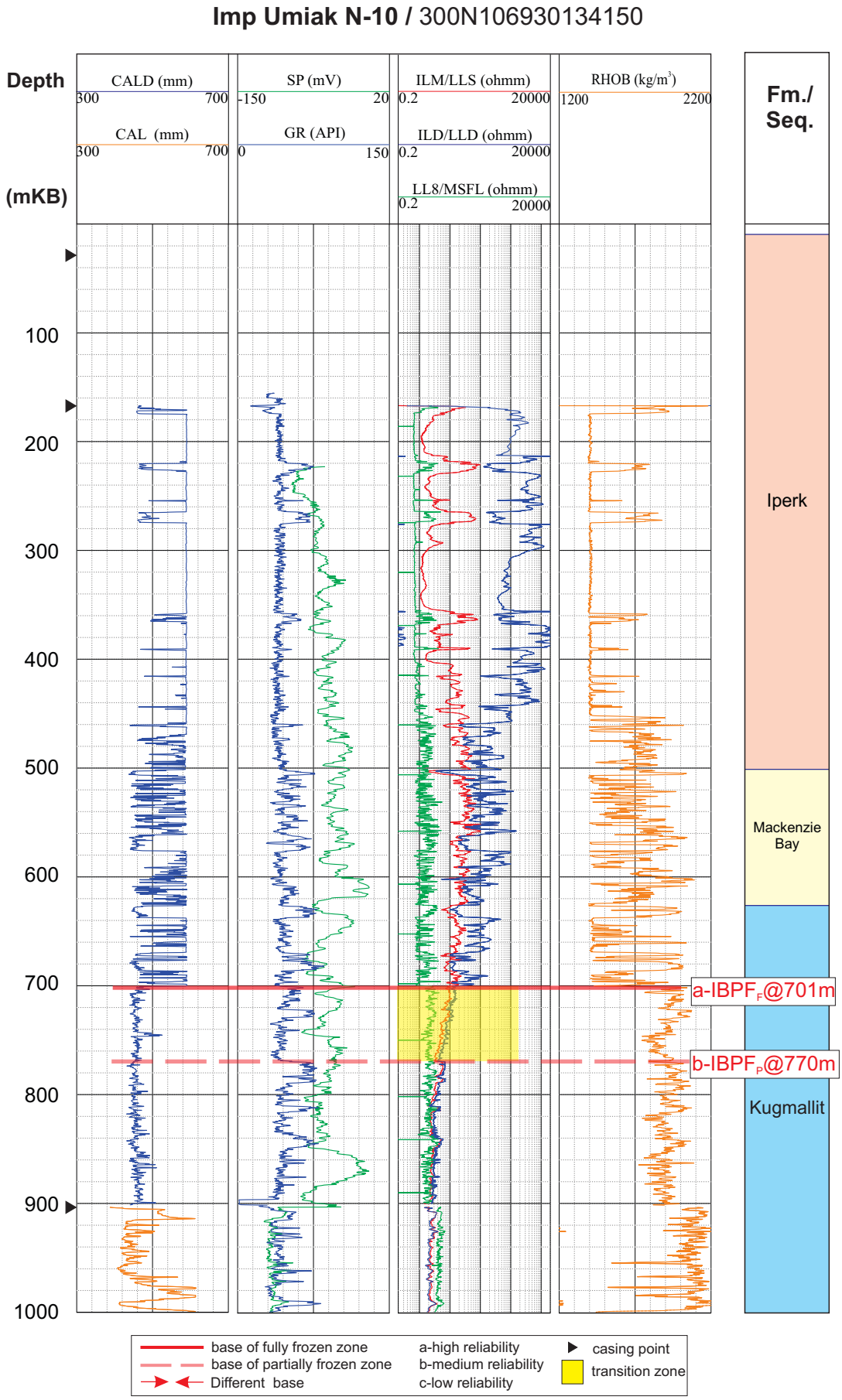

Figure 225. Determination of base of permafrost using geophysical logs for the Umiak N-10 well in the Beaufort-Mackenzie Basin.

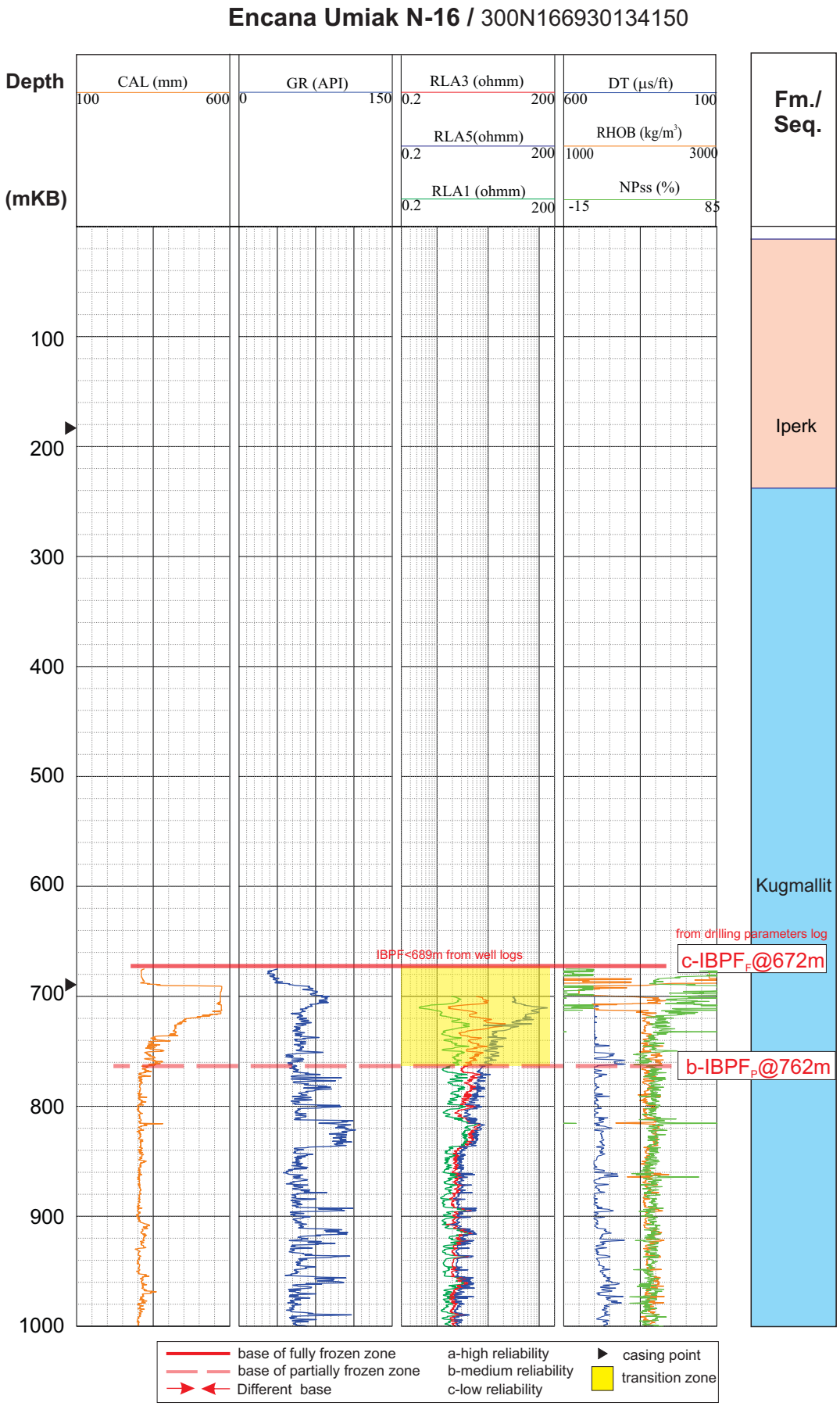

Figure 226. Log suite for the shallow interval of the Umiak N-16 well in the Beaufort-Mackenzie Basin, the possible fully frozen base of permafrost is from ROP (rate of penetration) data, the partially frozen base is from combination of well logs.

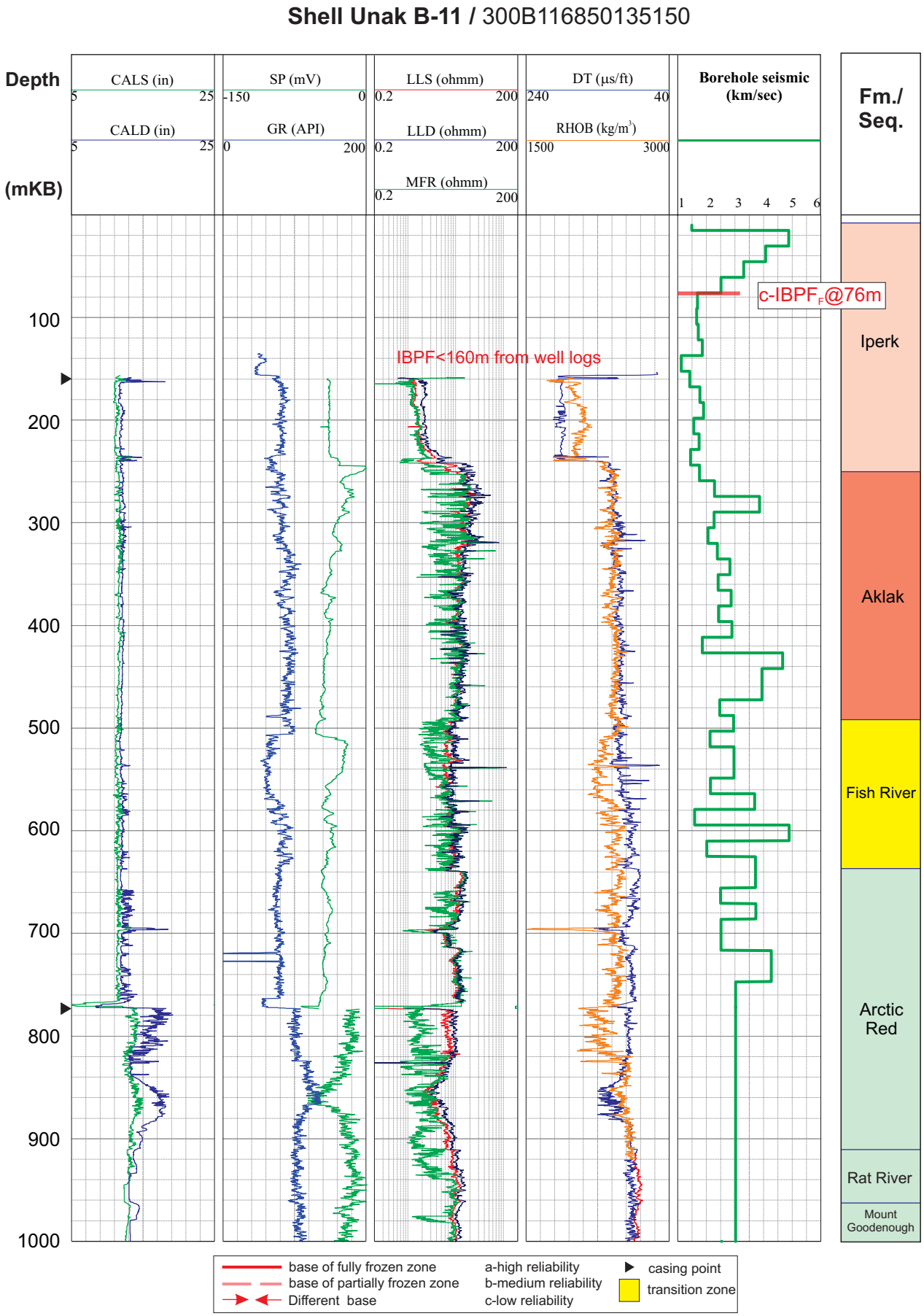

Figure 227. The base of permafrost is estimated from well seismic survey for the Unak B-11 well in the Beaufort-Mackenzie Basin.

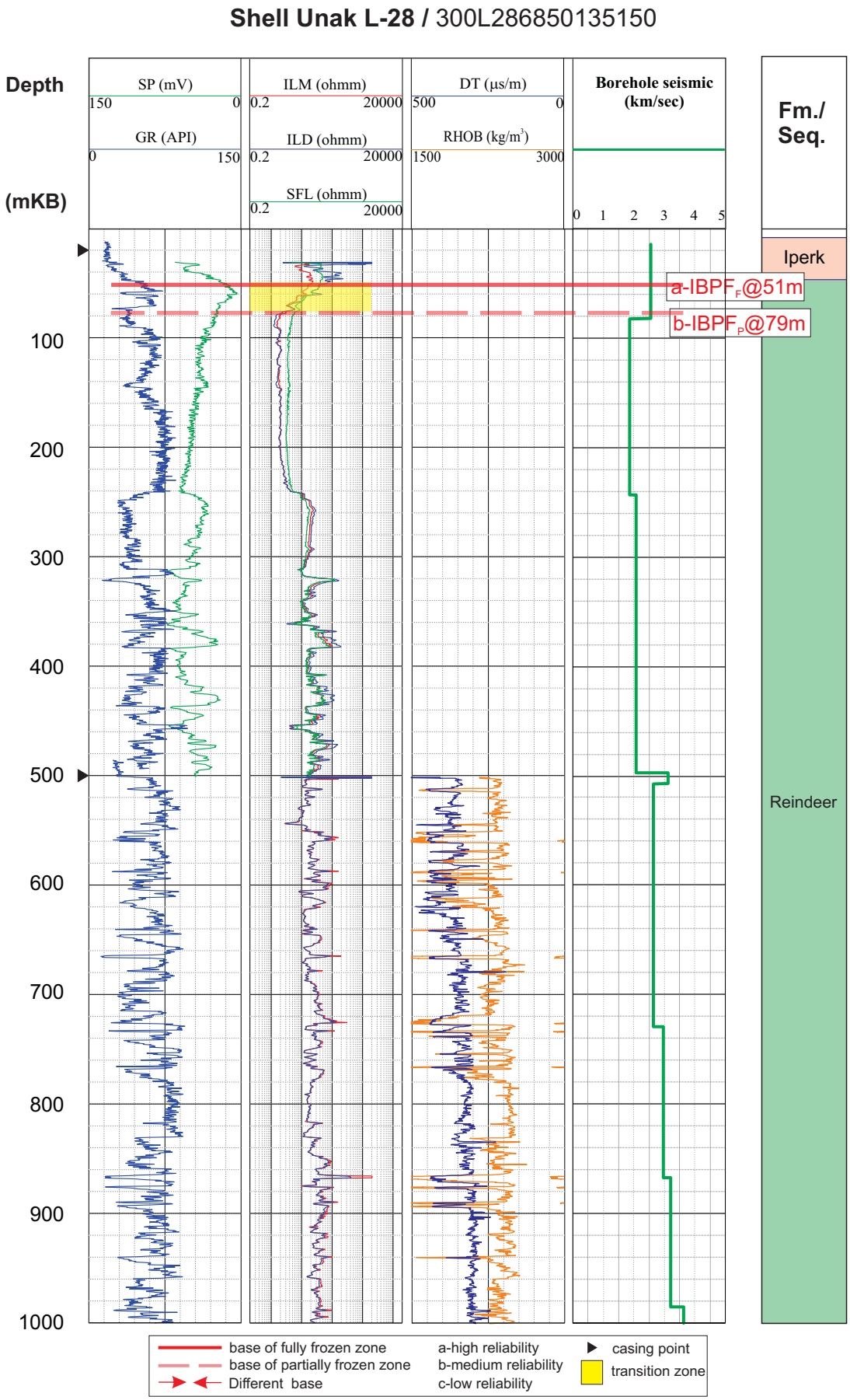

Figure 228. Determination of base of permafrost using well seismic survey and geophysical logs for the Unak L-28 well in the Beaufort-Mackenzie Basin.

Sun et al. Unark L-24/Unark L-24A / 300/302L246940134300

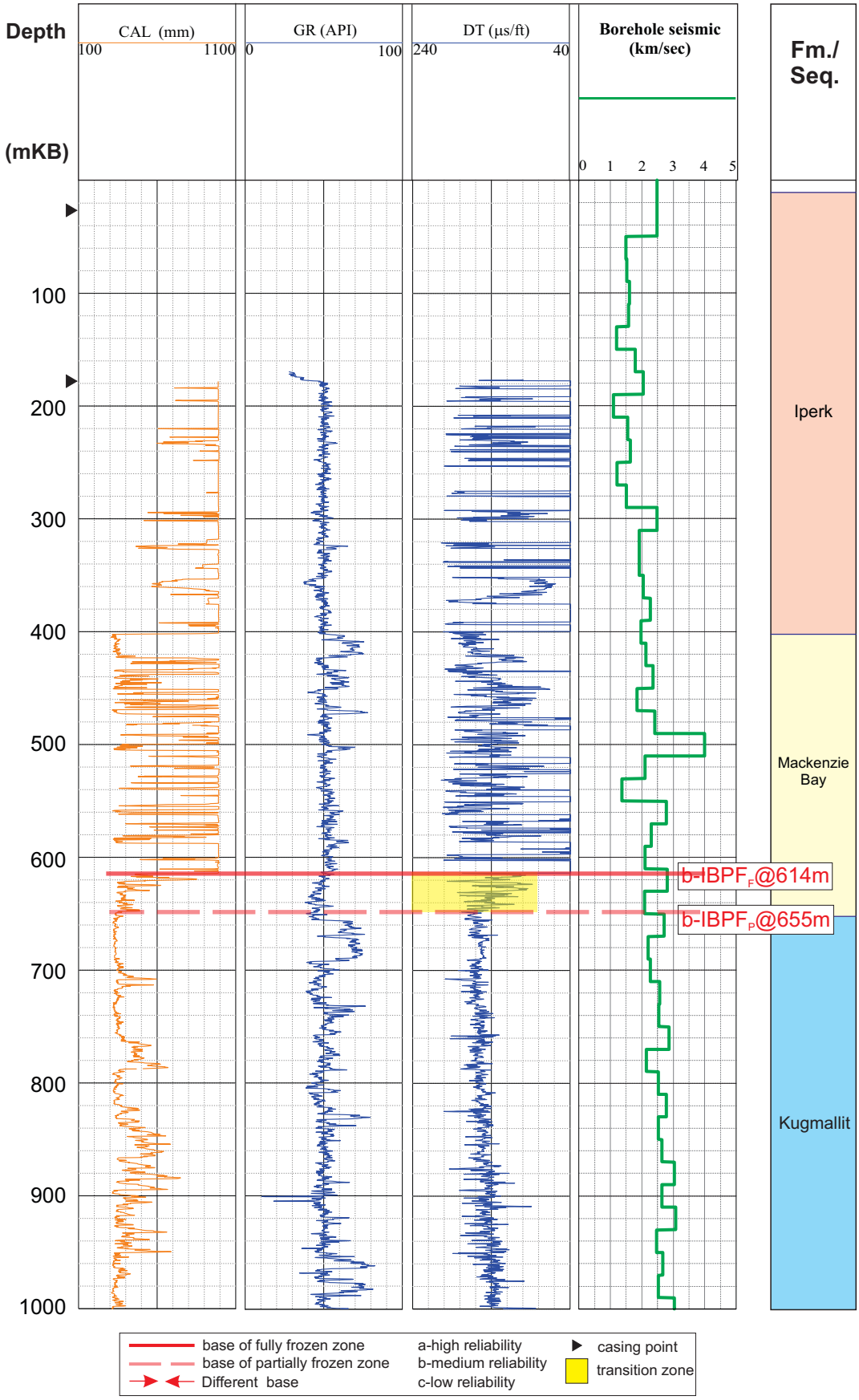

Figure 229. Determination of base of permafrost using well seismic survey and geophysical logs for the Unark L-24 well in the Beaufort-Mackenzie Basin.

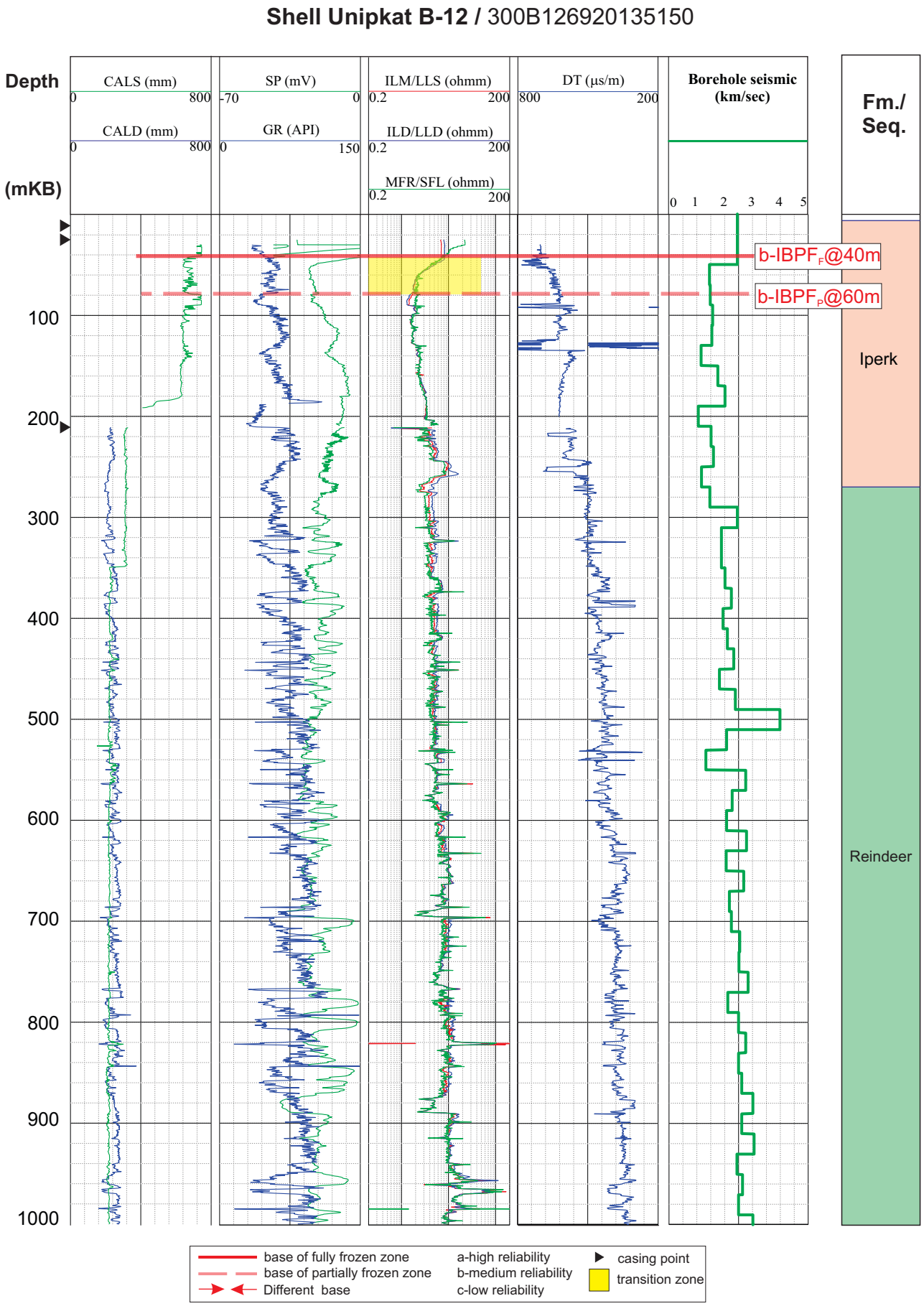

Figure 230. Determination of base of permafrost using well seismic survey and geophysical logs for the Unipkat B-12 well in the Beaufort-Mackenzie Basin.

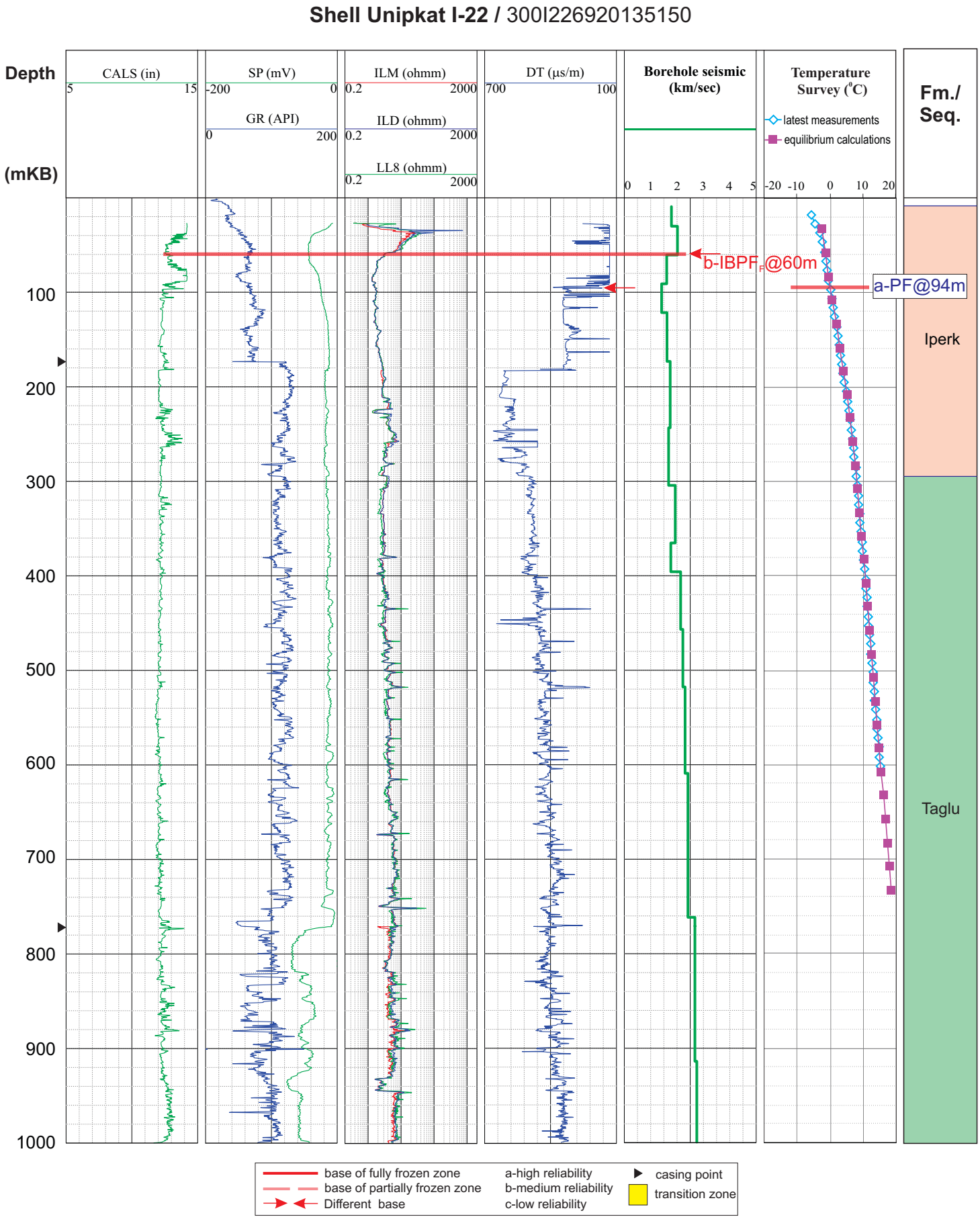

Figure 231. Determination of base of permafrost using temperature survey, well seismic survey and geophysical logs for the Unipkat I-22 well in the Beaufort-Mackenzie Basin.

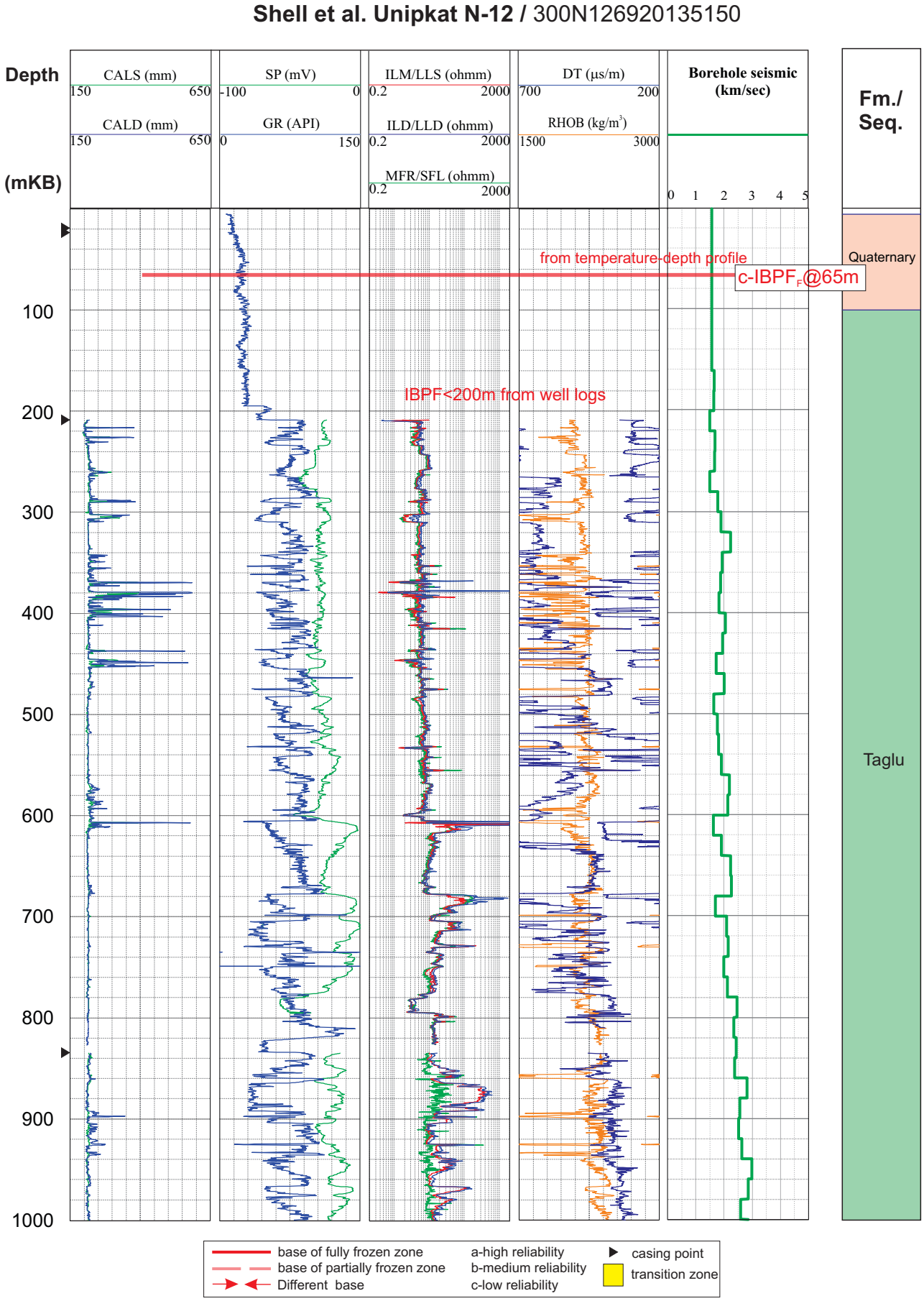

Figure 232. The base of permafrost is from temperature-depth profile due to lack of enough well logs for shallow interval for the Unipkat N-12 well in the Beaufort-Mackenzie Basin.

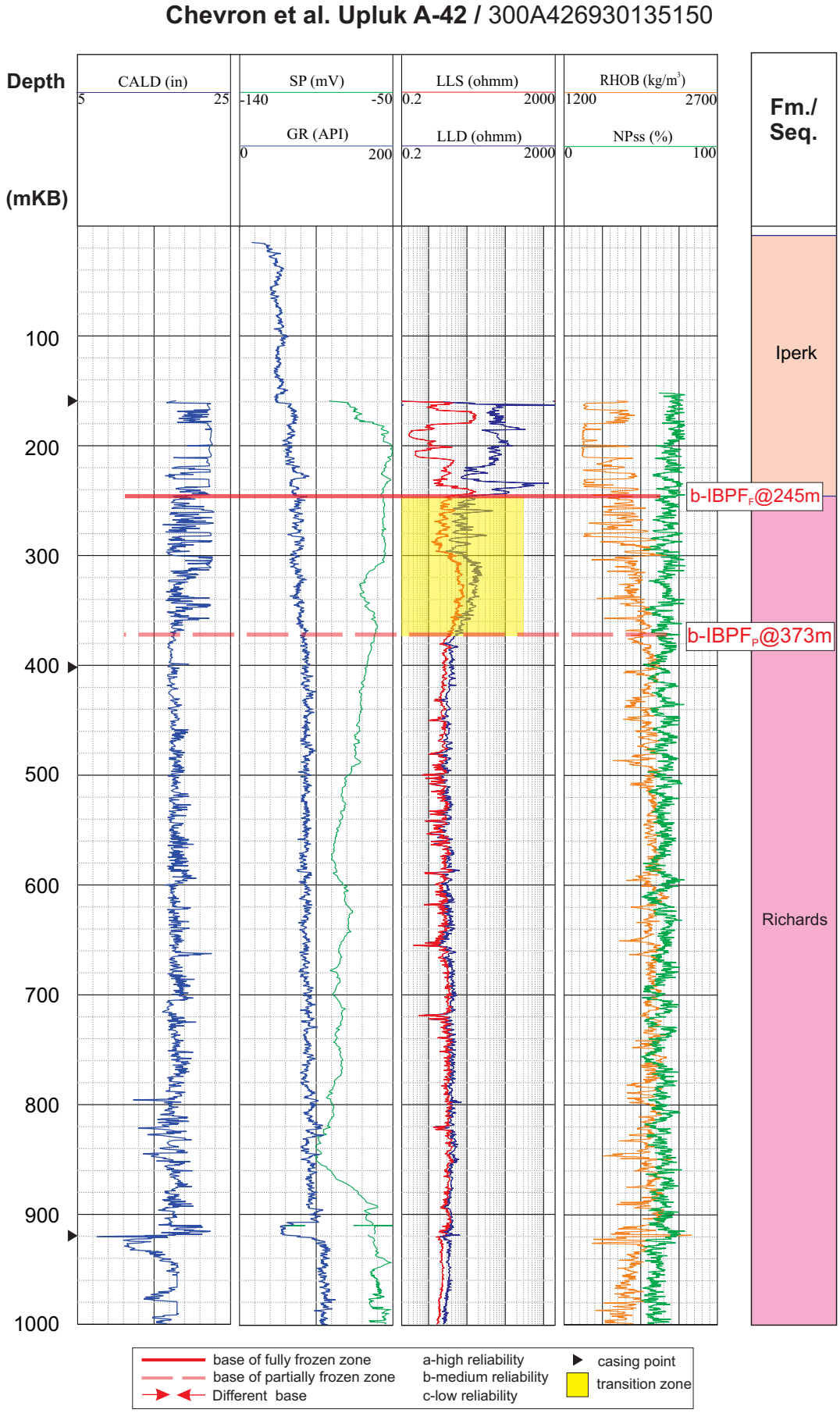

Figure 233. Determination of base of permafrost using geophysical logs for the Upluk A-42 well in the Beaufort-Mackenzie Basin.

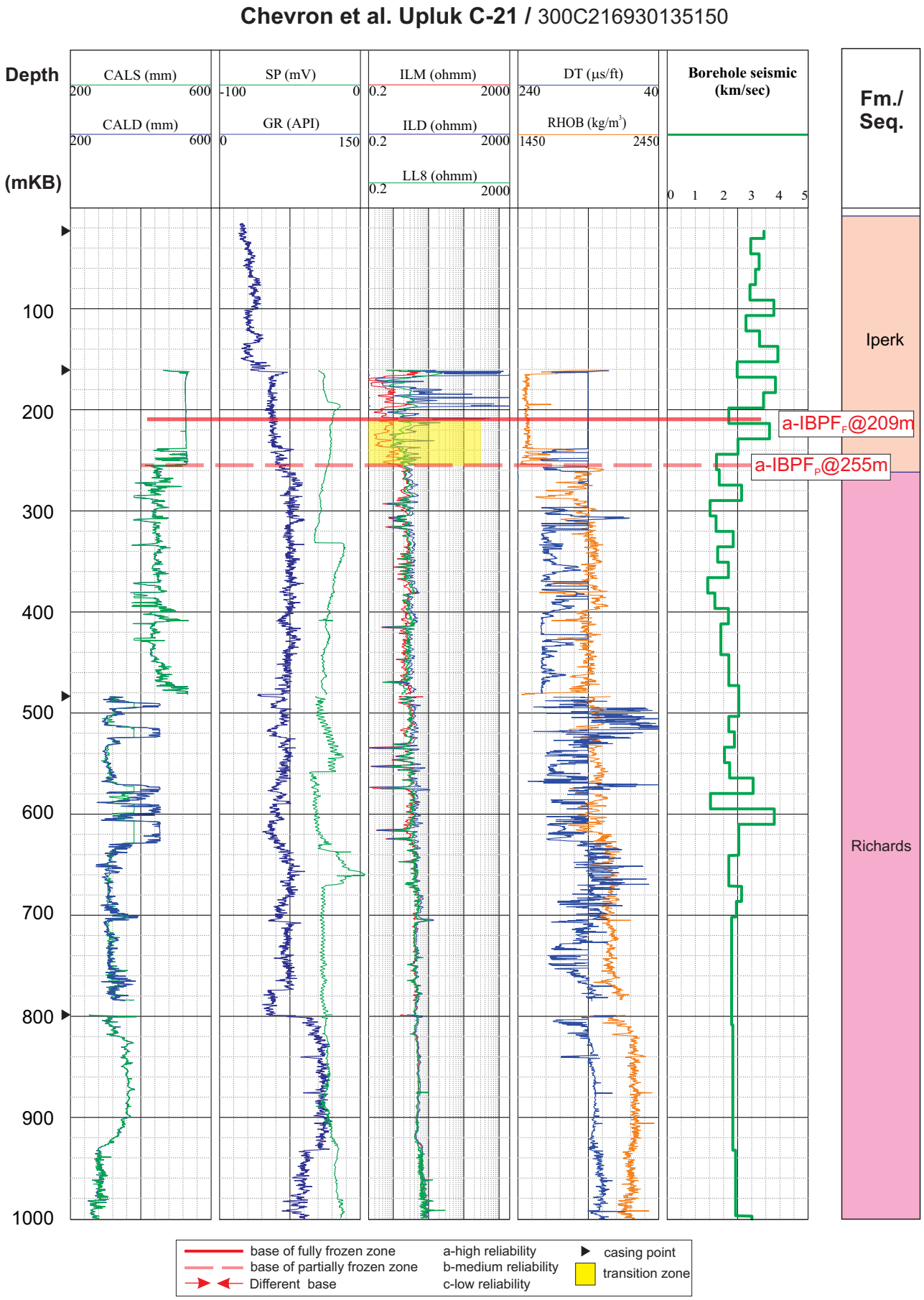

Figure 234. Determination of base of permafrost using well seismic survey and geophysical logs for the Upluk C-21 well in the Beaufort-Mackenzie Basin.

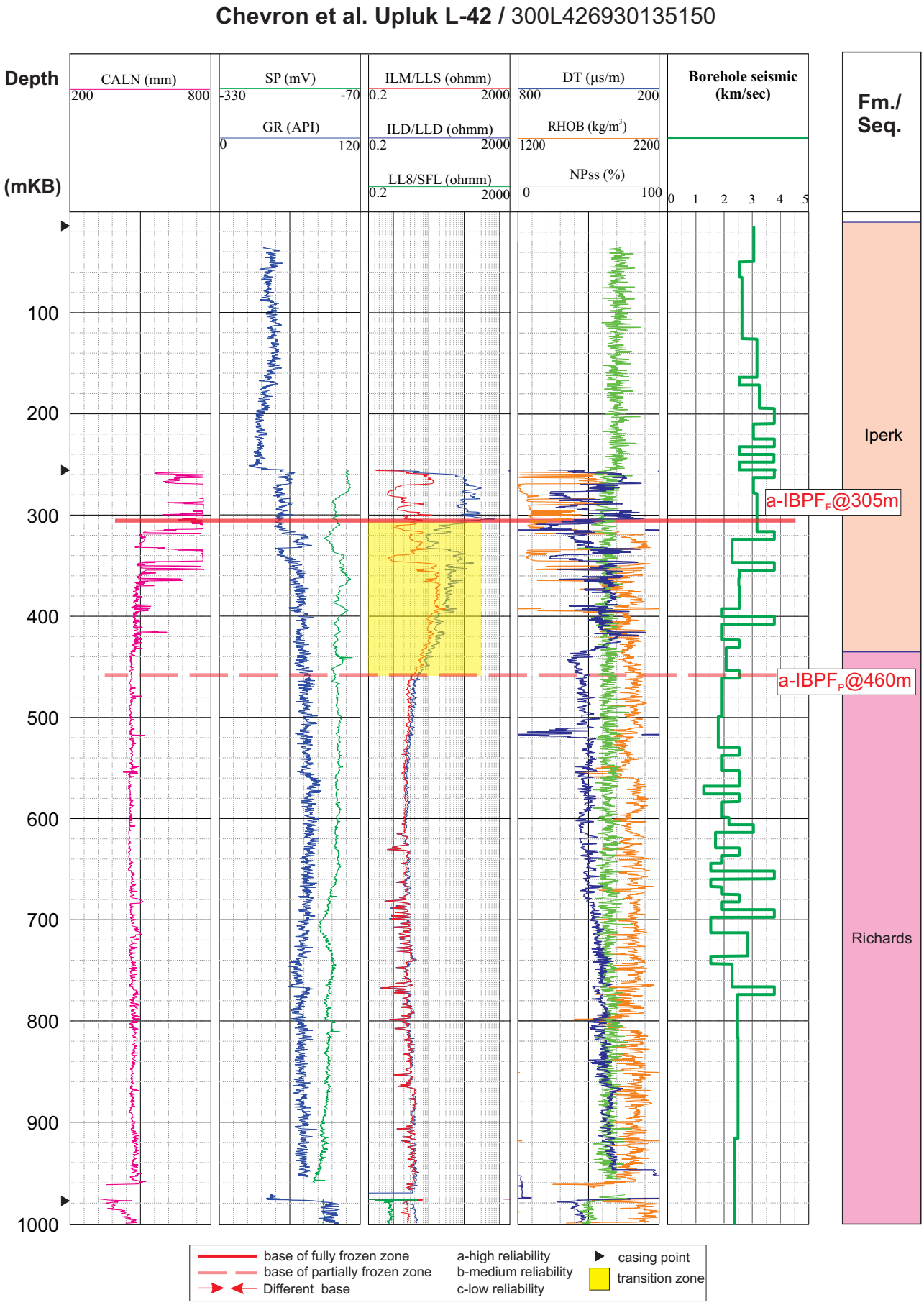

Figure 235. Determination of base of permafrost using well seismic survey and geophysical logs for the Upluk L-42 well in the Beaufort-Mackenzie Basin.

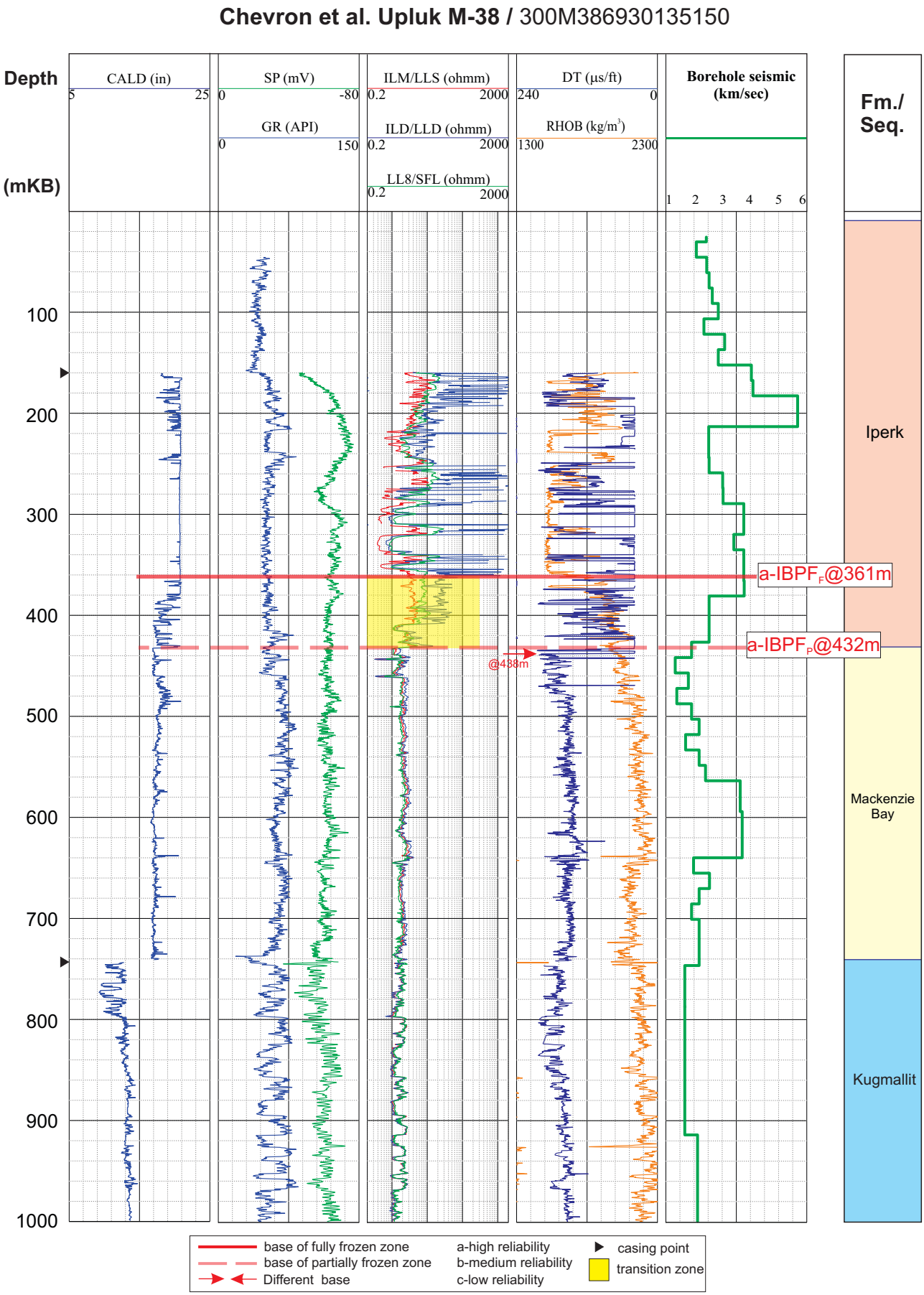

Figure 236. Determination of base of permafrost using well seismic survey and geophysical logs for the Upluk M-38 well in the Beaufort-Mackenzie Basin.

Dome et al. Uviluk P-66 / 300P667020132000

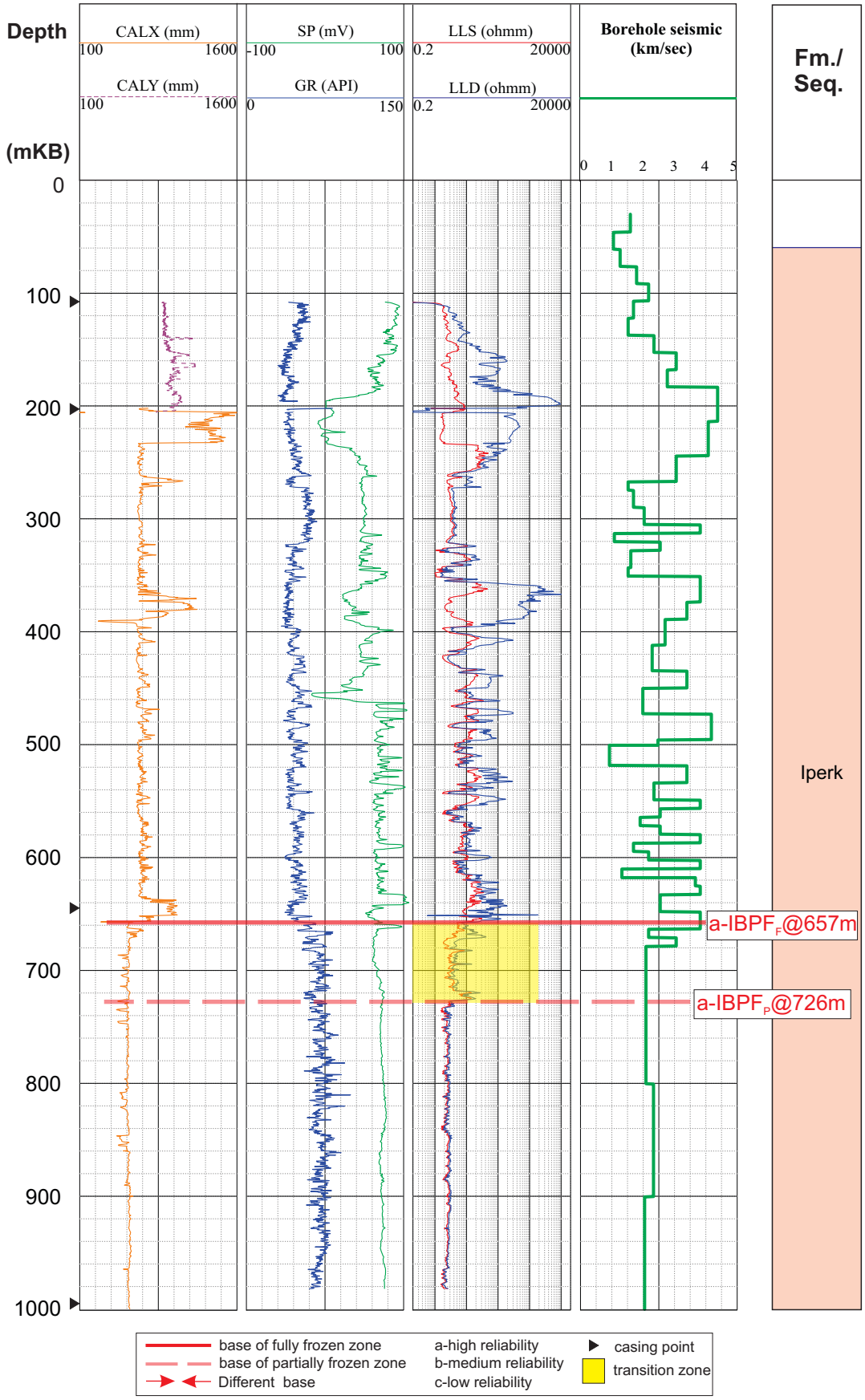

Figure 237. Determination of base of permafrost using well seismic survey and geophysical logs for the Uviluk P-66 well in the Beaufort-Mackenzie Basin.

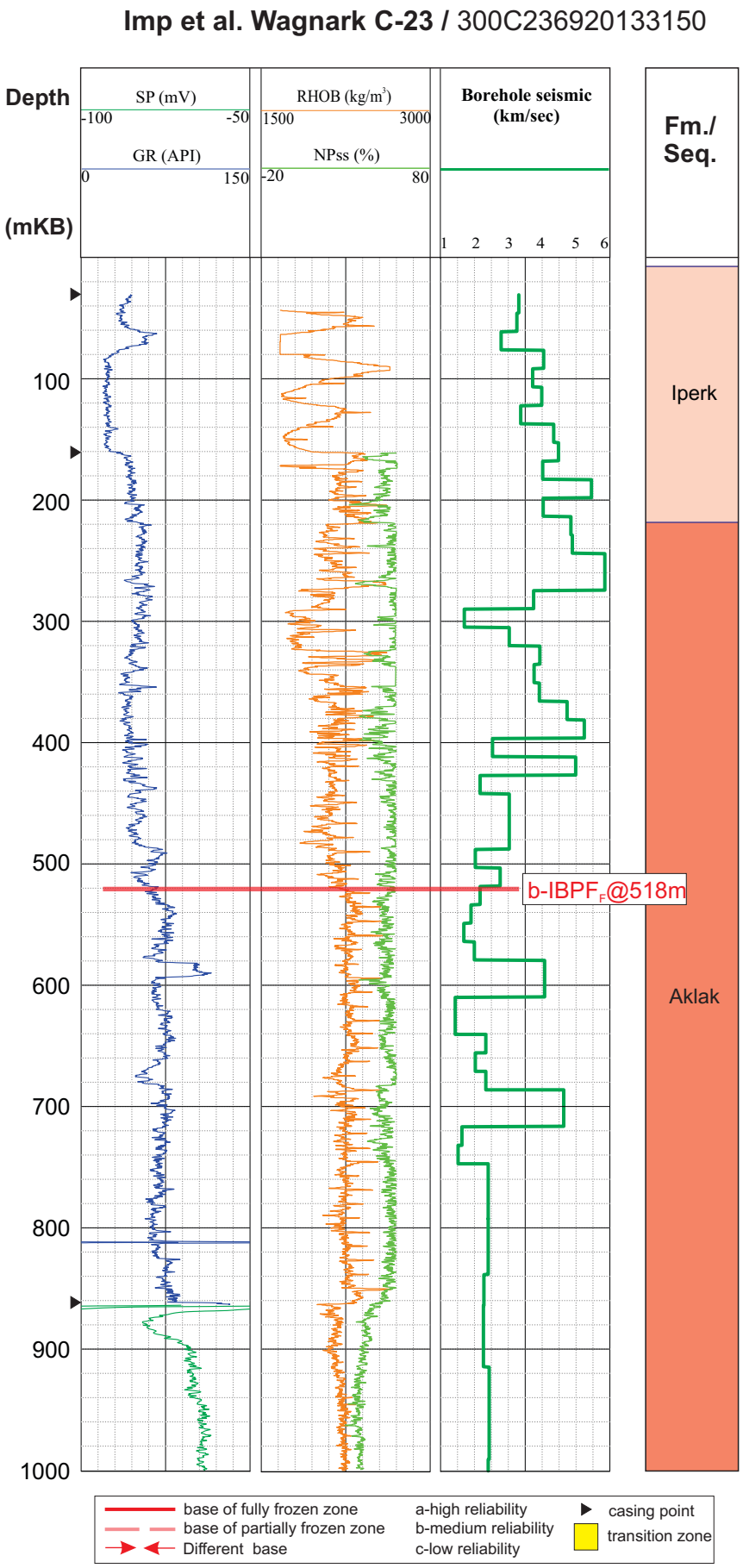

Figure 238. Determination of base of permafrost using well seismic survey and geophysical logs for the Wagnark C-23 well in the Beaufort-Mackenzie Basin.

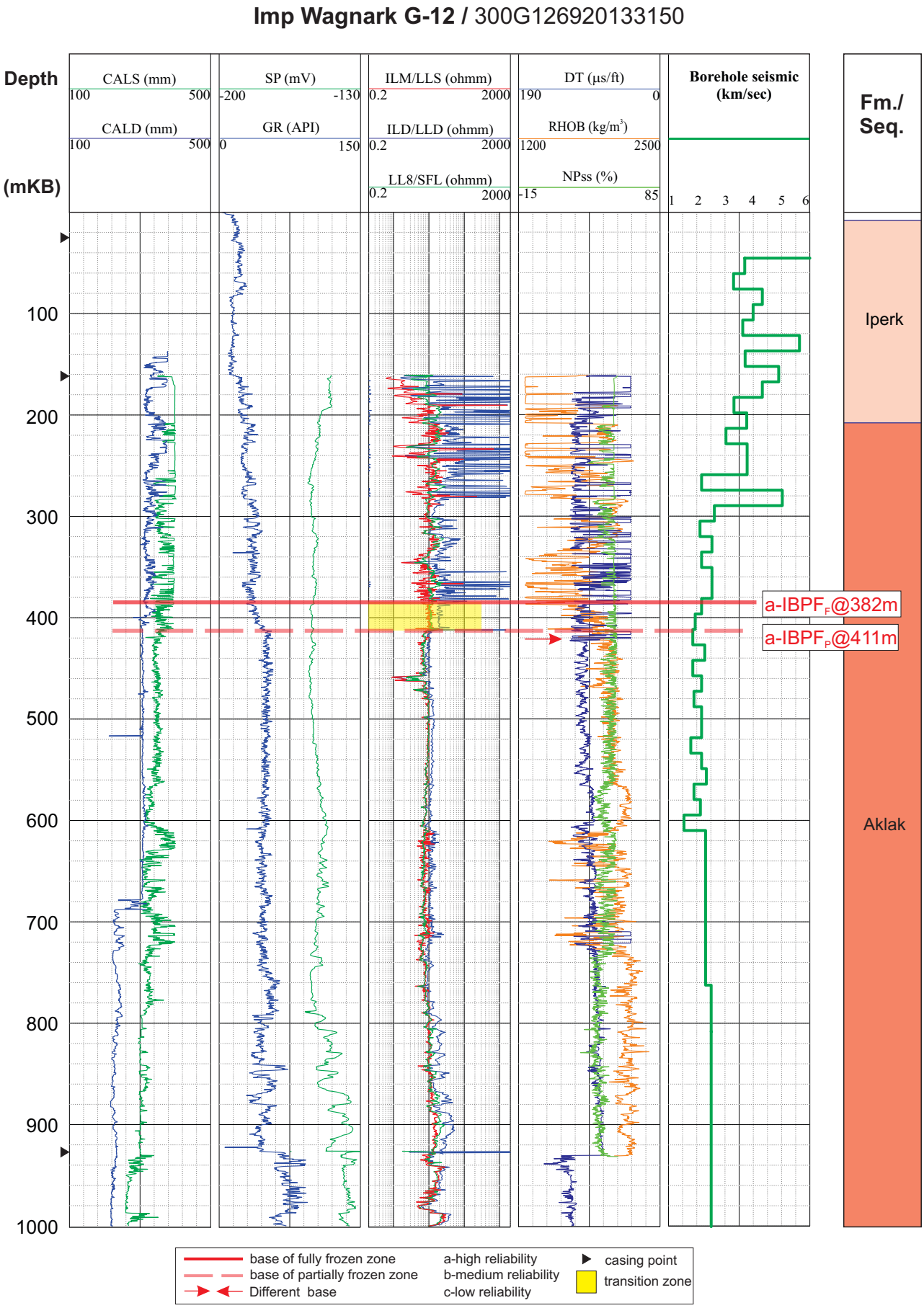

Figure 239. Determination of base of permafrost using well seismic survey and geophysical logs for the Wagnark G-12 well in the Beaufort-Mackenzie Basin.

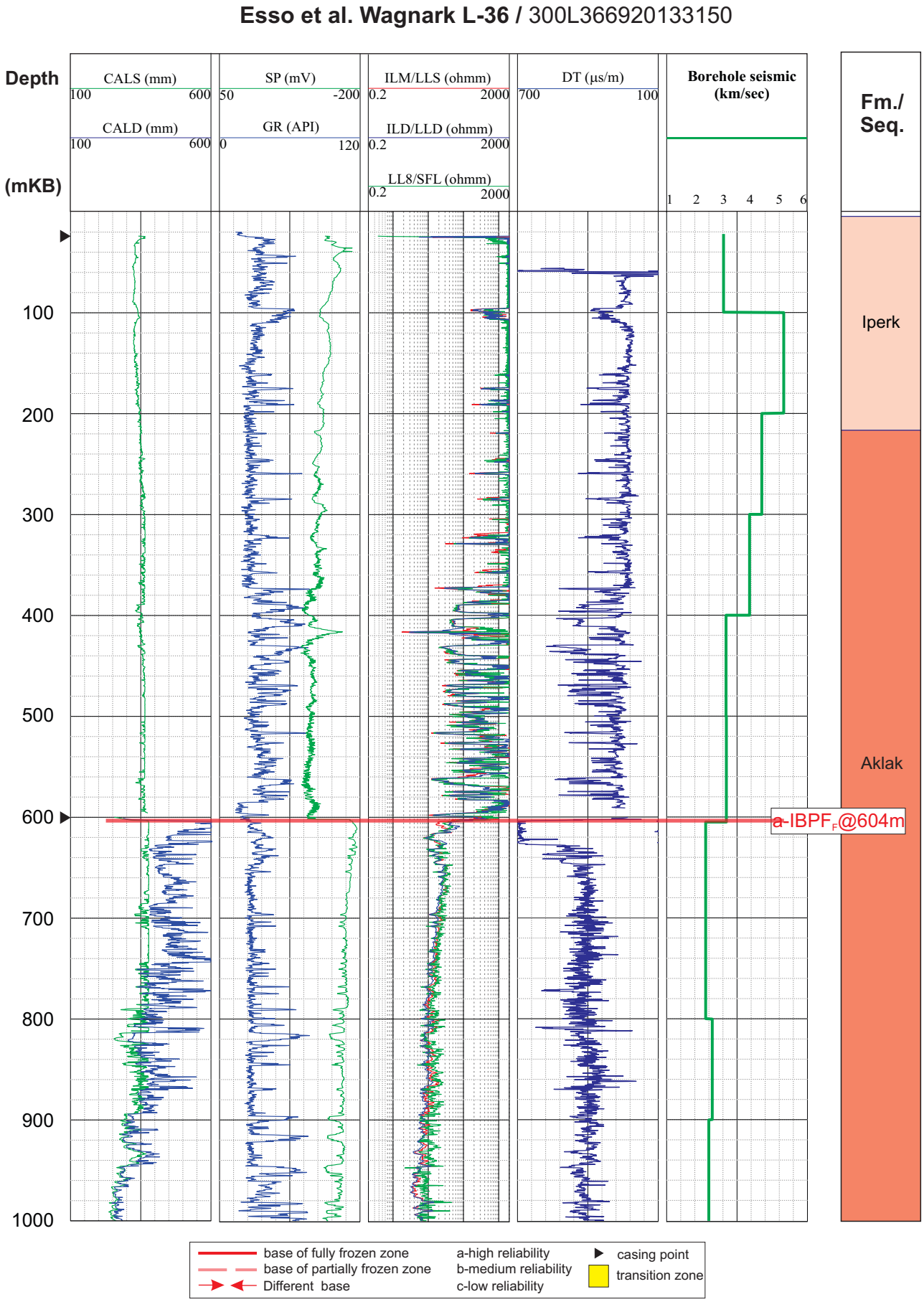

Figure 240. Determination of base of permafrost using well seismic survey and geophysical logs for the Wagnark L-36 well in the Beaufort-Mackenzie Basin.

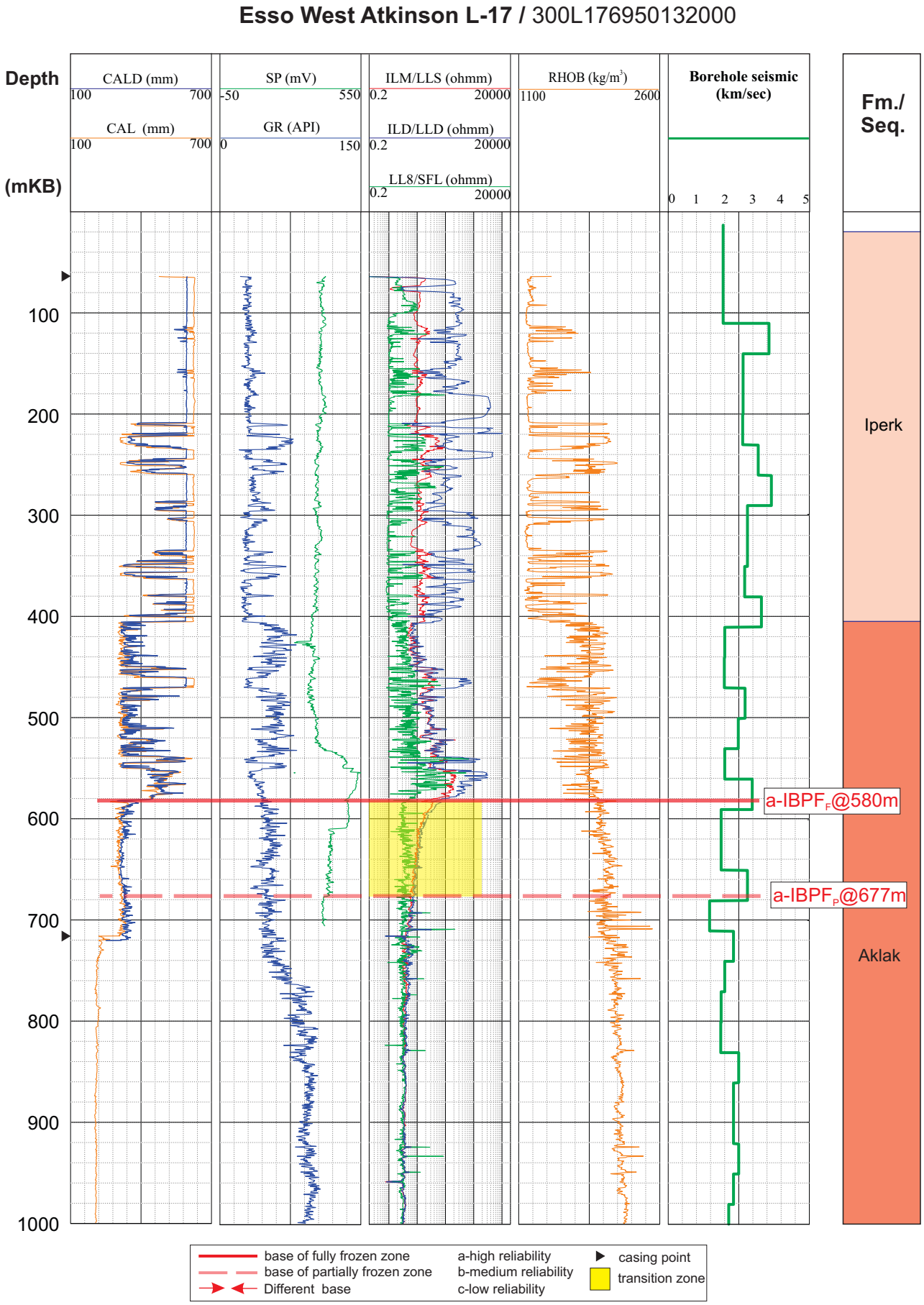

Figure 241. Determination of base of permafrost using well seismic survey and geophysical logs for the W. Atkinson L-17 well in the Beaufort-Mackenzie Basin.

Gulf et al. West Tarsiut P-45 / 300P457000136150

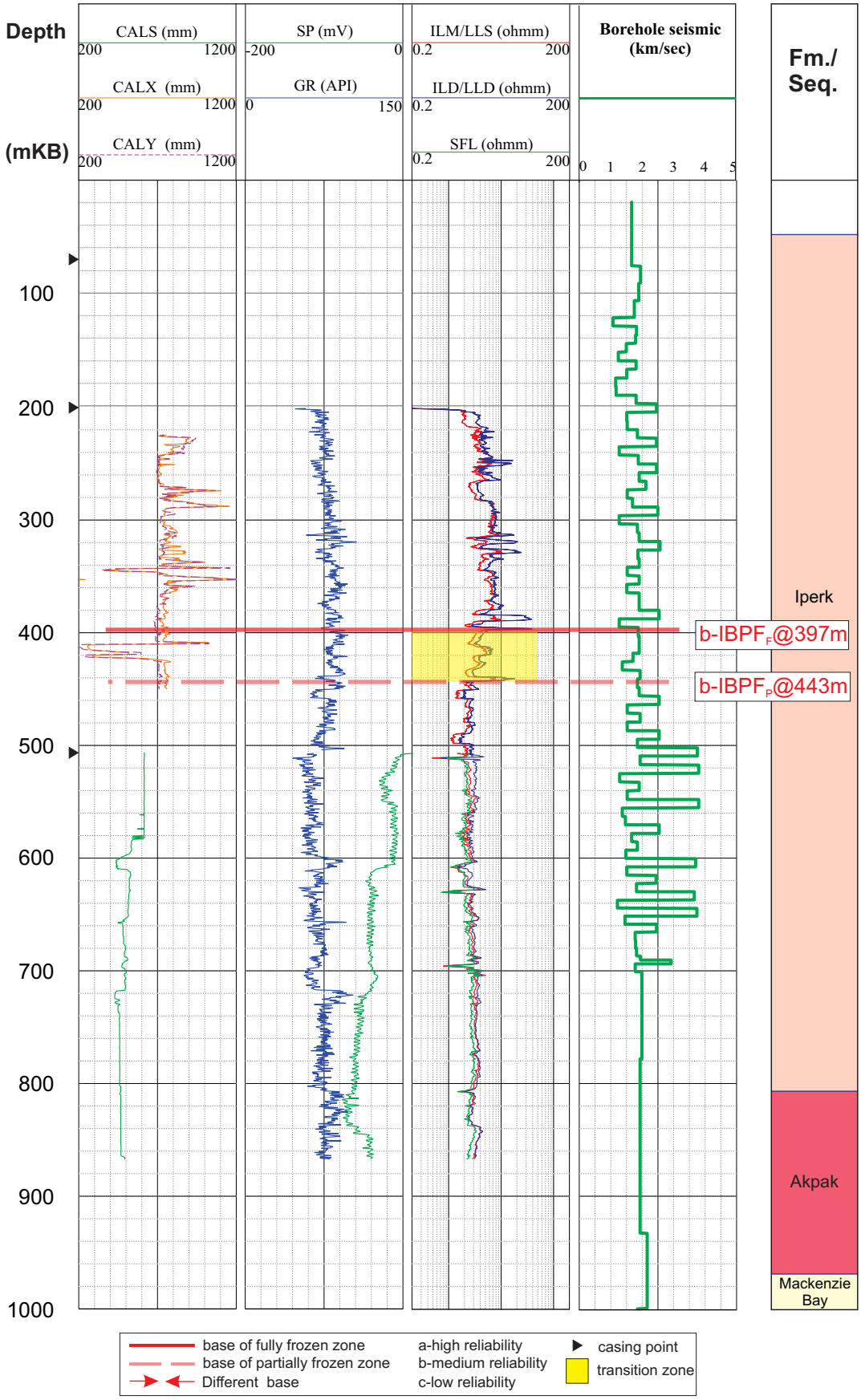

Figure 242. Determination of base of permafrost using well seismic survey and geophysical logs for the W. Tarsiut P-45 well in the Beaufort-Mackenzie Basin.

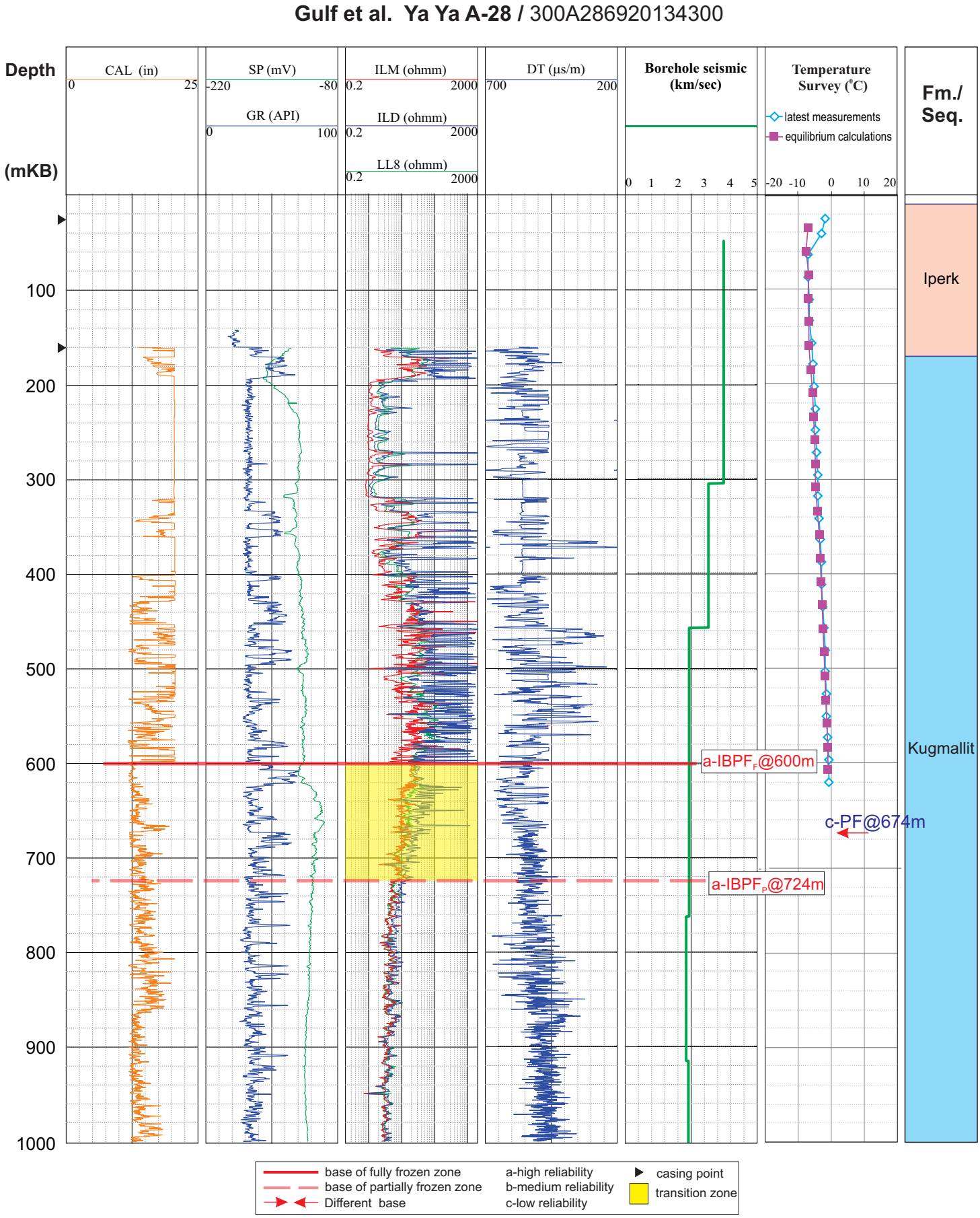

Figure 243. Determination of base of permafrost using temperature survey, well seismic survey and geophysical logs for the YaYa A-28 well in the Beaufort-Mackenzie Basin.

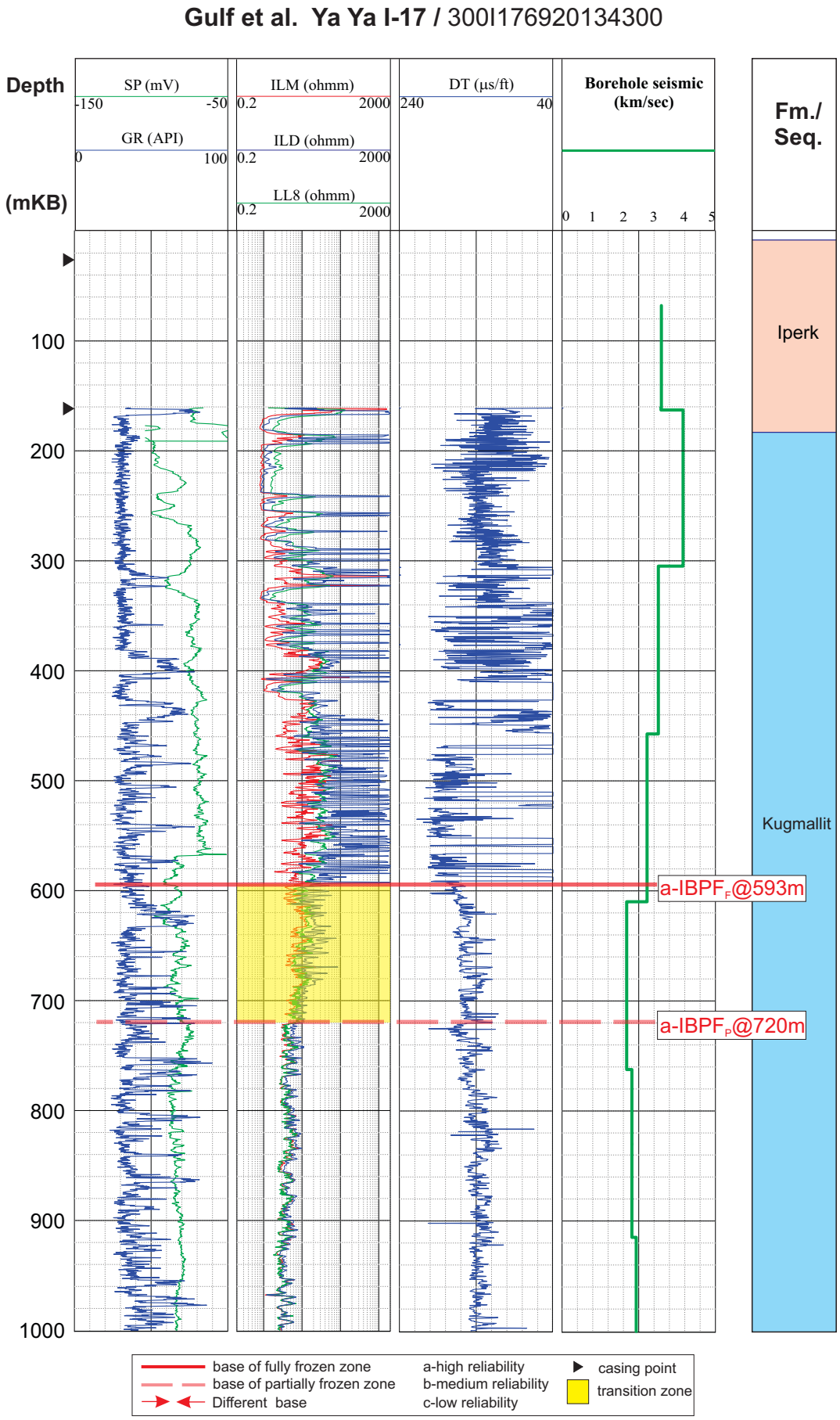

Figure 244. Determination of base of permafrost using well seismic survey and geophysical logs for the YaYa I-17 well in the Beaufort-Mackenzie Basin.

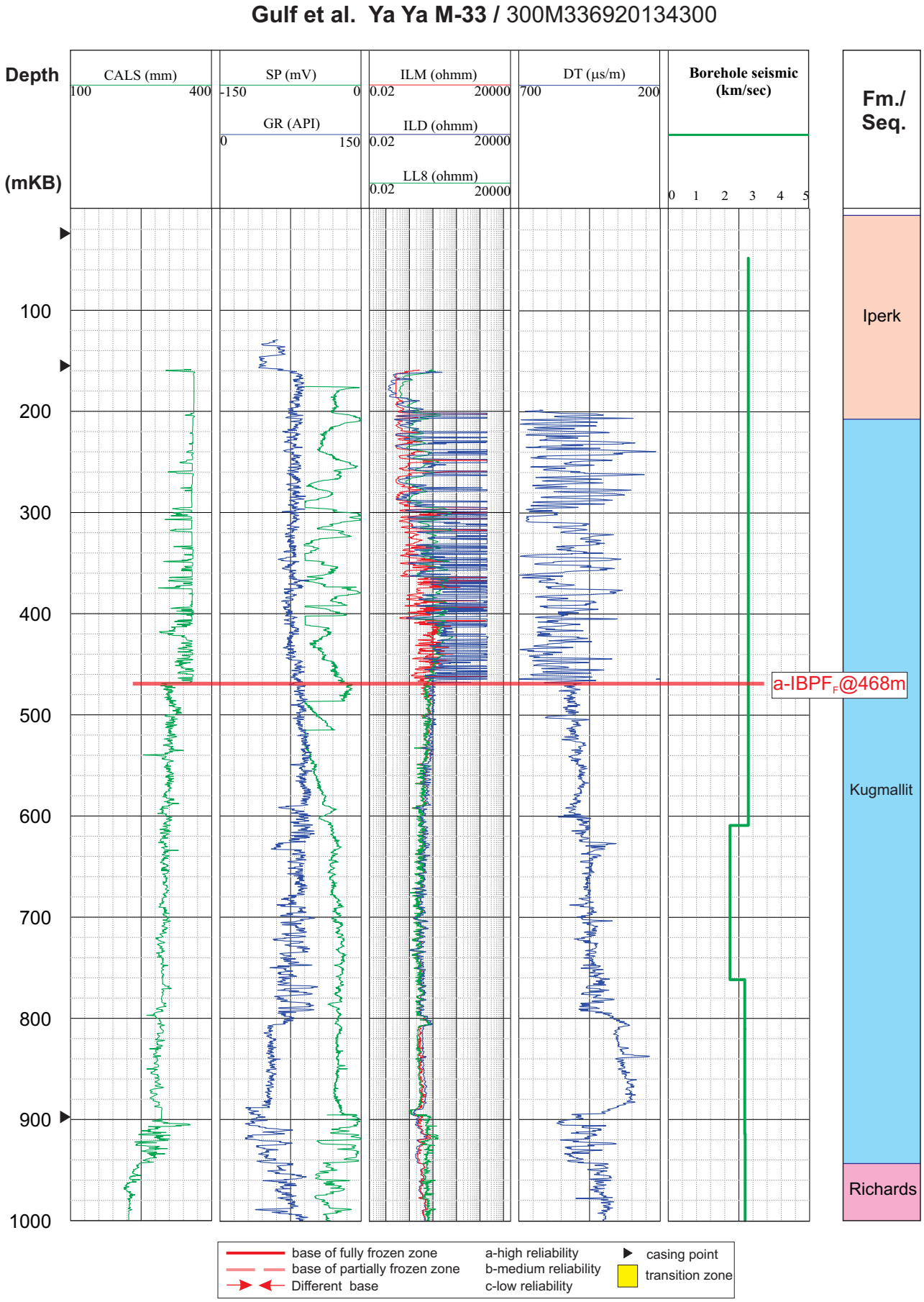

Figure 245. Determination of base of permafrost using well seismic survey and geophysical logs for the YaYa M-33 well in the Beaufort-Mackenzie Basin.

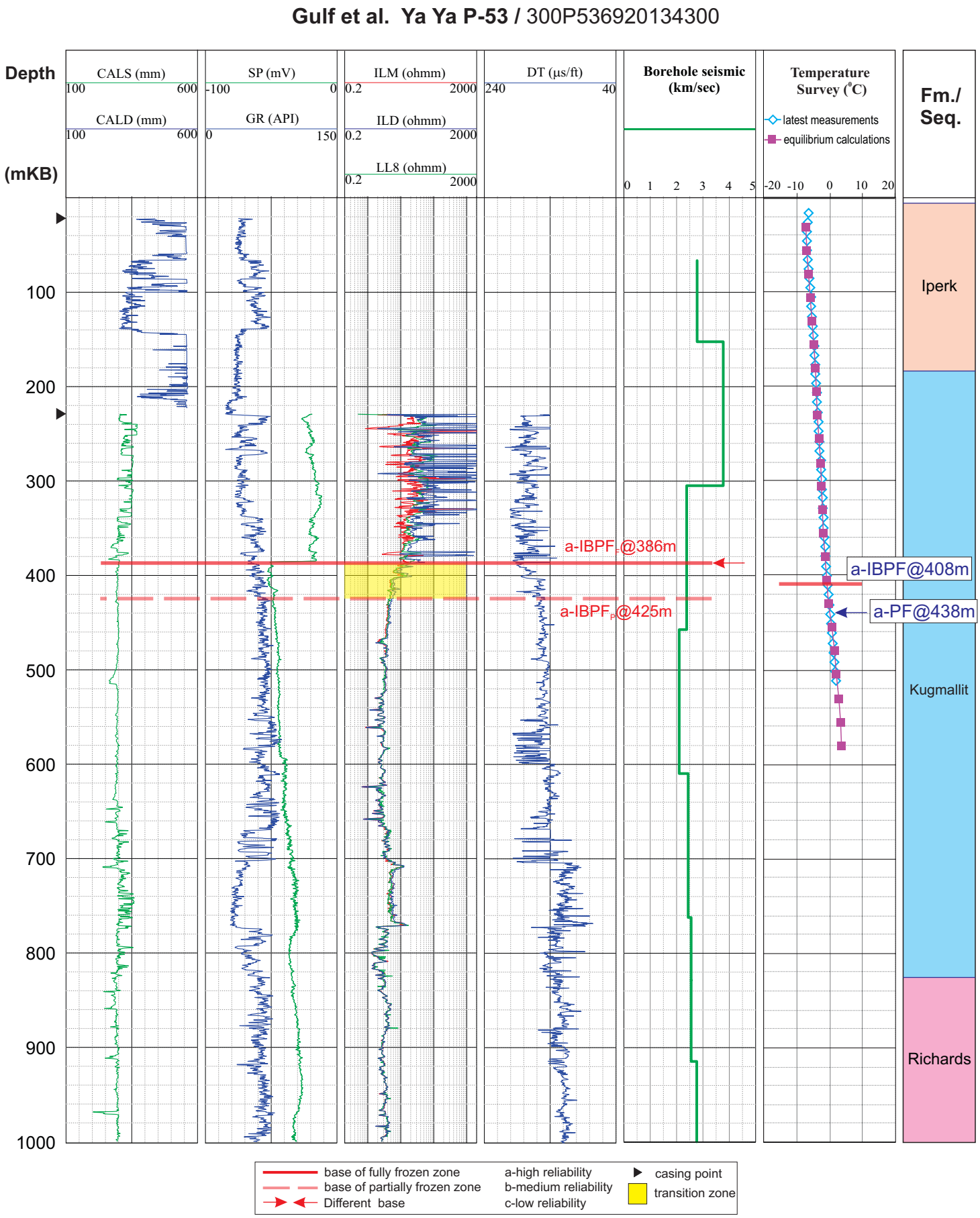

Figure 246. Determination of base of permafrost using temperature survey, well seismic survey and geophysical logs for the YaYa P-53 well in the Beaufort-Mackenzie Basin.